Faculty of Applied Sciences

Theoretical modeling of residue curve maps for a reactive distillation concept for the production of *n*-propyl propionate

Master Thesis Project

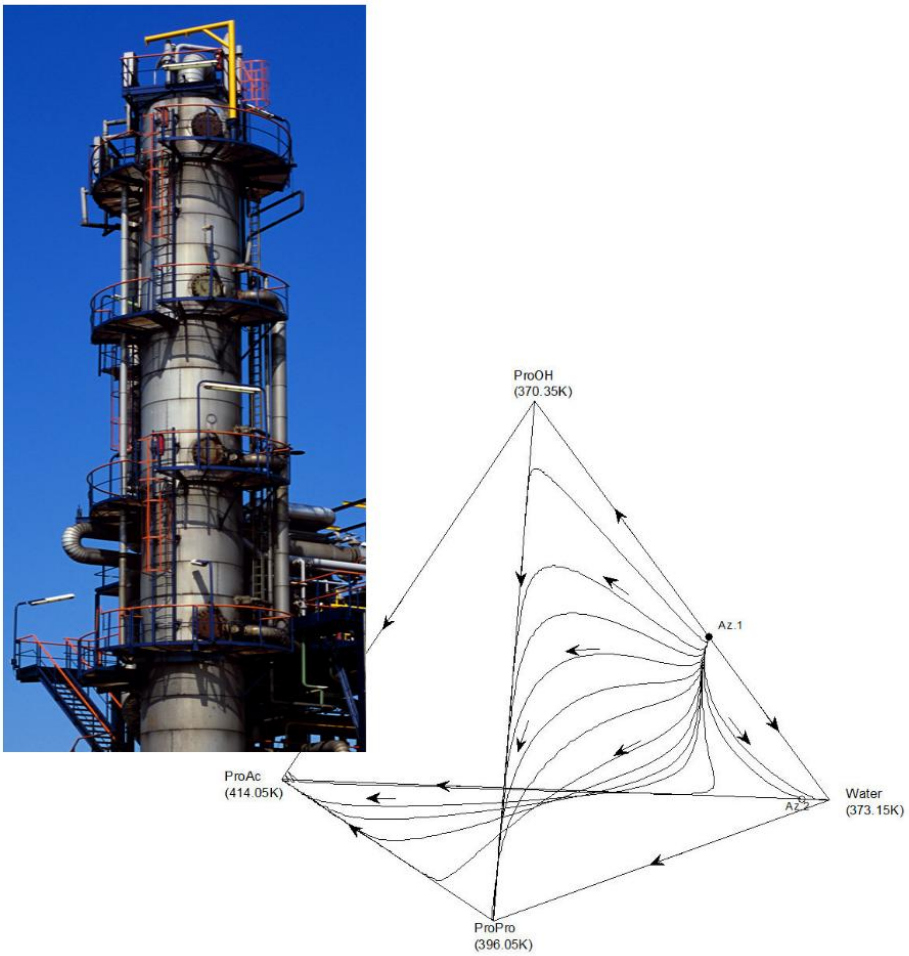

Name:	Henk Walpot		
Studentnumber:	1276875		
Programme:	Intensified reaction & separation systems		
Supervising Tutor:	G.D. Stefanidis	**Research Group:**	Process & Energy
2nd reviewer:	A.I. Stankiewicz	**3rd reviewer:**	T.J.H. Vlugt
Start date:	21-04-2011	**End date:**	20-12-2011
Subject to confidentiality agreements?		No	

Abstract

In this research residue curve maps are theoretically generated to assess the feasibility of a reactive distillation concept for the production of *n*-propyl propionate (ProPro). This product is a widely used solvent in industry and is synthesized by the heterogeneous catalyzed esterification reaction of 1-propanol (ProOH) and propionic acid (ProAc). The application of reactive distillation may result in higher yields, lower investment and operational costs and inherently safer processing. Thermodynamic and kinetic models are described for the quaternary reactive system, which agree well with experimental data from literature. The vapor-liquid equilibrium is modeled using the 'Gamma-Phi'-formulation where the activity coefficients are calculated using UNIQUAC and the fugacity coefficients are estimated using the method of Hayden-O'Connell. A pseudo-homogeneous approach is used to describe the reaction kinetics and Arrhenius-type of expressions are obtained for the chemical equilibrium constant and the reaction rate constant. The methodology and mathematical models for the residue curve maps are described for three scenarios: (1) non-reactive, (2) chemical equilibrium and (3) kinetically controlled. These cases show that the topology of the residue curve maps depends on the rate of reaction with respect to the rate of evaporation rate, which is included in the Damköhler (Da) number. Based on the reactive residue curve maps, the reactive distillation concept for the production of ProPro tends to be technically feasible using one single column where an excess of alcohol is used in the feed. The resulting process is able to produce pure ProPro at the bottom and an azeotropic mixture of ProOH and water at the top of the column. The separation of the top products by an additional separation step makes that ProOH can be recycled and high conversion levels can be obtained.

Preface

In the coming decennia the world is facing major energy and environmental issues induced by depletion of resources and global warming effects. The Internal Energy Agency (IEA) predicts in its World Energy Outlook of 2011 that the total energy demand increases by one-third from 2010 to 2035. This is mainly due the rapid growth of the world's population, increasing global wealth and emerging economies in the world. In 2011, the world welcomed the seven billionth human being and it is expected that the eight billion is reached before 2025 according to the United Nations. Furthermore, the IEA predicts the number of passenger vehicles doubles to 1.7 billion in 2035 and that cumulative CO_2-emissions exceed three-quarter of the total since 1900. The consequences are rising energy prices, scarcity of fossil fuels and enhanced greenhouse-effects due to the pollution of the atmosphere. Therefore, significant actions have to be taken in order to prevent this or as the IEA stated: ”If we don't change direction soon, we'll end up where we're heading”[1]. Alternative energy sources like gas and coal are short-term solutions and the processing of these raw materials still does not solve the environmental issues. More sustainable energy sources like solar energy, wind energy and biomass energy are still not technically and practically feasible to be applied on a large scale. Therefore, besides searching for alternative and renewable energy sources, it is also essential to develop innovative methods and technologies that reduce the energy consumption and waste production directly.

The increasing costs for energy consumption and waste treatment are significant factors in current chemical process design developments. It is essential for the chemical industry to adapt by being more energy efficient and reducing their emissions and waste production. Process Intensification (PI) is a methodological technique that has proven to be effective in innovating chemical processing[2]. When applied successfully, the PI principles generate intensified processes that are more energy efficient, have lower operational and investment costs, reach higher yields and selectivity's and are inherently safer than their predecessors. The methodology focuses on four approaches in spatial, thermodynamic, functional and temporal domains, which are used to realize four generic principles[3]. These approaches refer to every aspect in chemical processing from molecular to macro scale. Some interesting outcomes of PI are microreactors, reactive separation processes, high gravity applications and the use of microwaves as alternative heating method[4].

Index

Chapter 1. Introduction

Reactive distillation is one of the most successful technologies emerged from process intensification research applied in industrial practices. This innovative process technology forms a synergy between the unit operations for reaction and distillation that results in several advantages in terms of efficiency and safety. However, the process complexity is significantly increased and the feasible operation window is reduced which results in more complex process design methodologies. This chapter gives a general introduction to this research by first describing the fundamentals of reactive distillation. Then the design of this type of processes is described with emphasis on the feasibility study for process concepts. The residue curve mapping technique is described in more detail as it is used as a fundamental feasibility method through this thesis. At the end of this chapter the objective and significance of this research is formulated and the structure of this thesis is outlined.

1.1 Reactive distillation

In chemical process industry many processes are based on the principle of carrying out reaction and separation sequentially in separate process units. The integration of these chemical functions into a multifunctional unit could drastically increase the performance of these processes[5]. A successful integration technology is the reactive distillation column which is a hybrid operation that combines the reaction and distillation task into one piece of equipment. This technology can be either used to enable separation of close-boiling or azeotropic mixtures[6] or to enhance the efficiency of chemical reactors. The second and more interesting application of reactive distillation involves addition of *in situ* separation to a chemical reactor. This is particular interesting for equilibrium-based chemical reaction processes since chemical equilibrium limitations can be overcome. Due to the possibility of *in situ* separation, it is possible to remove one of the products out of the reactive zone which causes the equilibrium conversion to move towards the products side. This way higher conversion levels and selectivity's can be achieved. Furthermore, heat integration can be applied between the heat of reaction and the energy input for distillation. These advantages of reactive distillation result in increased process efficiency, economic benefits such as lower investment and operational costs and reduction of health, safety and environment risks[5].

The first patent for the concept of reactive distillation already appeared in the 1920's by Backhaus[7]. Although, it would take until the 1980's before the first industrial application was commercialized. The first applications were introduced in the production of ethers and esters of which the synthesis of methyl acetate by Eastman Chemicals is considered as the most representative example. Here, the conventional process consisting of 11 different process steps and 28 major pieces of equipment was effectively replaced by a single multifunctional reactive distillation column (figure 1.1). This resulted in 80% less investment costs and the energy consumption was reduced by ca. 85% for the production of methyl acetate[8]. The success of these applications resulted in a major interest of the industry for the use of reactive distillation in other types of processes. Therefore much research is done on the application of reactive distillation in other types of reactions like acetalization, hydrogenation, alkylation and hydration. This resulted in commercialized processes for the production of MTBE, TAME, cumene and ethylbenzene[5,9] for example.

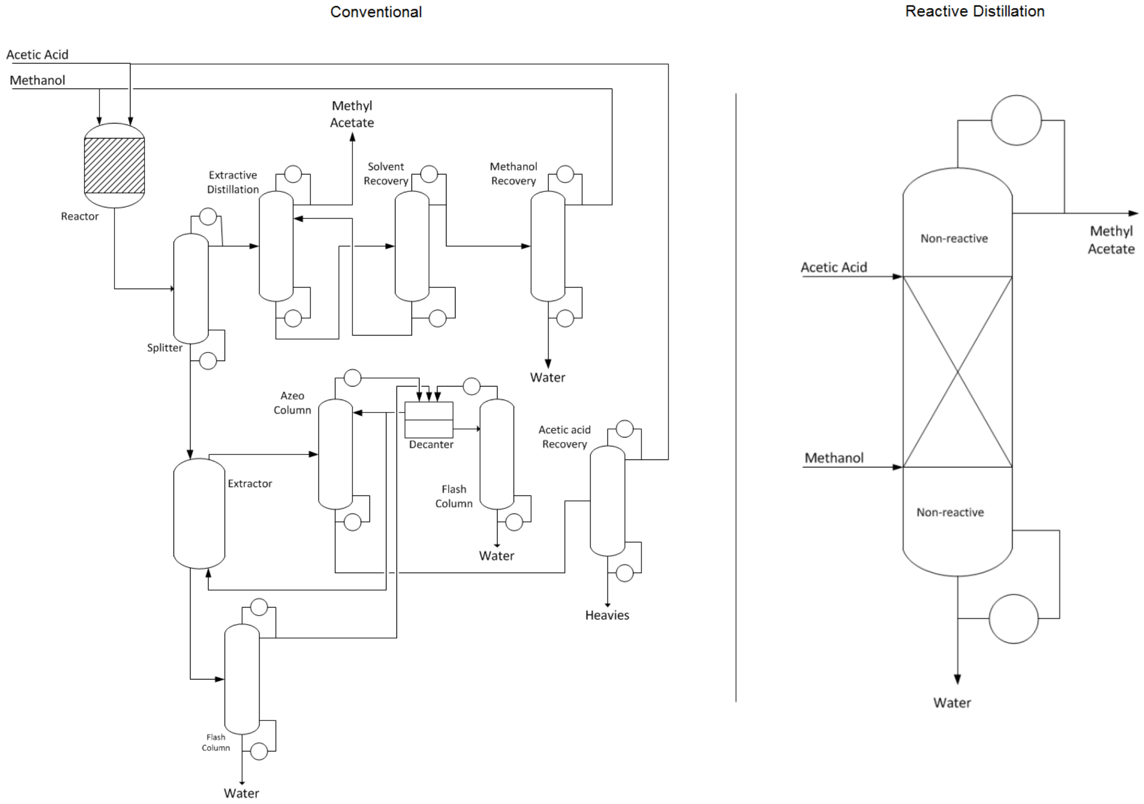

Figure 1.1. Eastman Chemical’s conventional (left) and reactive distillation (right) methyl acetate process

The combination of reaction and separation processes in a single unit makes that the design and operation of this hybrid process is far more complex than the individual operations. This is already evident from the fact that the first application was installed 60 years after the first patent was published. First, it is essential that the conditions, temperature and pressure, for reaction and distillation are in the same operating window. This implies that at the operating conditions the relative volatility between reactants and products is large enough to be able to separate those and that the rate of reaction is reasonably high such that no large residence time is needed for the reaction. Furthermore, the introduction of a chemical reaction into a distillation process leads to complex interaction between thermodynamics, kinetics and transport phenomena. These interactions have large influences on the design parameters of the unit and lead to complex process dynamics, which include multiple steady states and the presence of reactive azeotropes. The presence of additional variables, the nonlinear interaction between phases and reaction and the coupling between heat and mass flow complicates the design and modeling of these columns. Therefore, the design issues in case of reactive distillation are far more complex than those involved in conventional distillation units which pose a major challenge on the design of these systems.

1.2 Feasibility study for reactive distillation concepts

The art of chemical process design is to develop an economical, safe and environmentally responsible process where raw materials are converted into valuable products. This is done by finding efficient process configurations, unit equipment sizes and optimal operating conditions. The boundaries of the design are specified by the product specifications and the characteristics of the feed. The methodology for chemical process design can be divided in several phases following the Stage-Gate^{TM} process development strategy[10] which are shown in figure 1.2. A process design starts with a certain concept of which first the feasibility is assessed. Only feasible processes are continued in the development phase where the design is getting more detailed and equipment are sized. Then at the end of the process design the equipment is built and the process is started for production.

Figure 1.2. Stage-Gate^{TM} Product-Development Process (SGPDP).

As shown in figure 1.2 the preliminary stages of the process design sequence is formed by the feasibility study of interesting process concepts. This task is not trivial and requires the development of specialized design tools like computational methods, algorithms and procedures. Due to the coarse level of detail, the design tools in the conceptual phase should be powerful enough to screen the feasibility within a large design space.

Reactive distillation processes are very promising in substituting conventional liquid phase reaction processes. However this technology is not suitable for any kind of process or type of reaction. Therefore, assessing the feasibility of these process concepts forms an important area in current and future research and development activities. The development of reliable tools and design strategies is therefore an important feature of these kinds of researches. In the latest years several systematic design methods for reactive distillation have emerged, which can be roughly divided into two categories; graphical and numerical methods[11].

The graphical design tools make use of graphical information to determine the feasibility of reactive distillation concepts. These diagrams are mainly constructed by means of theoretical models, which generate residue curves or distillation lines. The behavior of these lines shows valuable information about the characteristics of the studied process. There are several methods which are mainly divided into two groups. The first group refers to a graphical approach based upon thermodynamic-topological analysis of distillation lines as described by Giessler et al.[12]. They use static analysis to determine the feasibility of reactive distillation columns operating in the kinetic regime and with large internal flows. The other graphical method is based upon the use of transformed composition variables which were first developed by Barbosa et al.[13,14]. The transformed compositions have the similar properties as the mole fractions in conventional distillation. The assumption here is that the reaction rate is infinitely fast which make that the reaction is at equilibrium at any instant in time. Later this method was extended by Buzad[15] for describing processes which are kinetically controlled which resulted in the so-called “fixed-point” method.

The second category of feasibility study, numerical methods, is more based on analyzing the physiochemical data of the process. They are supported by computational subroutines and take into account important elements of an overall design strategy, like types of phase equilibrium, number of components and occurrence or not of chemical reactions on a given stage. Ciric and Gu[16] developed a mixed integer nonlinear programming (MINLP) method for determining the number of trays, holdup volumes, feed tray location and reflux ratios.

The most widely used method in the preliminary design of a reactive distillation processes is the residue curve mapping technique. These maps can be constructed either experimentally or theoretically based on simple batch distillation. The strength of this technique lies in the fact that it is conceptually simple and only little physical data of the process is required to generate these maps theoretically. One needs to specify the feed composition, a phase equilibrium model and the chemical kinetics. The largest limitation of this technique is that only systems can be visualized with a maximum of four components due to the limitation of graphical representation in a 3-dimensional space. Another drawback is that accurate thermodynamic and kinetic data are required to correctly describe the residue curves for a reactive distillation process.

1.3 Residue curve maps

The residue curve mapping technique is a graphical method for the flow-sheet development and preliminary design of multi-component (reactive) distillation processes. It provides a powerful tool to represent relevant properties of the system, particularly those aiming to predict feasibility of processes where highly non-ideal and azeotropic mixtures are involved. Residue curve maps (RCM’s) were first described by Schreinemaker[17] in 1901. These maps are a collection of individual residue curves which are the locus of the compositions of the residual liquid in time, as vapor is boiled off from a simple distillation still. This corresponds to the liquid composition along a distillation column with infinite number of stages and operating at total reflux. At first, RCM’s were used in the conceptual design of conventional distillation processes involving highly non-ideal azeotropic mixtures. Later this technique was extended and it appeared that it was also very useful in the design of reactive distillation processes.

Single residue curves can be obtained relatively easy by performing a simple Rayleigh batch distillation experiment were no trays, packing or reflux are involved. During the experiment the composition of the liquid residue in the still is continuously analyzed until the last drop is vaporized. Then by repeating the experiment for various starting compositions of the liquid a collection of residue curves can be obtained from which the RCM can be built. However, RCM’s can also be obtained mathematically by specifying a limiting number of physical parameters and solving the mass balance of the simple batch experiment analytically.

The topology of a RCM is mainly determined by the number and location of singular points, called vertices, in the system[18,19]. The physical meaning of these fixed points is that from this point forward in time the composition of the liquid residue does not change. Therefore, these vertices correspond to the location of the pure components and the (reactive) azeotropes of the system. A system can have multiple azeotropes between two, three or more components depending on the number of components and the thermodynamic characteristics of the system. There are two types of singular point: nodes and saddles, which jargon comes from the stability theory of ordinary differential equations. The nodes represent the vertices where the residue curves either start or end. The saddles are the points which are first approached by the residue curves and then they move away from it. These vertices are never reached by one of the residue curves. This terminology is more clearly seen in figure 1.3. Usually the nodes are the high- and low-boiling vertices while the saddles are intermediate boiling vertices. The nodes in a system are either stable or unstable. A node where all residue curve converging to is called a stable node, which can be compared with the low point of a valley in which a rolling ball finds a stable position. Conversely, a node where all residue curves deviating from, is called an unstable node since it is like the top of a peaked mountain from which a ball rolls towards a stable position[20].

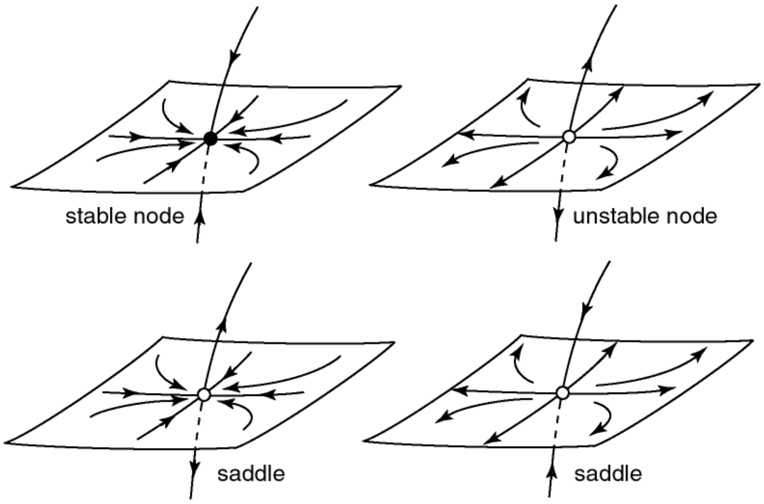

Figure 1.3. Possible configurations of singular points: stable node, unstable node or saddle

The presence of multiple singular points in a RCM could lead to the division of the diagram into separate distillation regions. This makes that residue curves follow different trajectories with different unstable and/or stable node depending on the starting composition of the liquid residue. These different regions are bounded by so-called separatrices which connect two or more singular point in the composition space. Each distillation region is characterized by having one unstable and one stable node between which the residue curves are located[21]. The distillation regions are an important factor in the feasibility of certain (reactive) distillation processes since these boundaries determine whether it is possible to obtain the pure products from the process. For the separation of homogeneous mixtures by simple distillation these separatrices cannot be crossed unless they are highly curved.

The RCM characteristics discussed above are made clearer by the example shown in figure 1.4. This figure shows the RCM for the non-reactive ternary system of acetone, chloroform and benzene. The RCM is shown in a triangular composition plane where each corner resembles a pure component vertex. This ternary system contains one maximum-boiling binary azeotrope between acetone and chloroform which is indicated in figure 1.4. All residue curves in the figure either start in the pure component acetone or chloroform vertex and end in pure benzene. This makes that pure acetone and chloroform are unstable nodes and that pure benzene is a stable node and that the binary azeotrope is a saddle point in the system. The direction of the residue curves, indicated in the figure by arrows, is always in the direction of increasing temperature and time. The presence of the binary acetone/chloroform azeotrope makes that the RCM is divided into two distillation regions which are separated by the distillation boundary between the binary azeotrope and the pure component benzene vertex. This separatrice is indicated in the RCM by the dotted line.

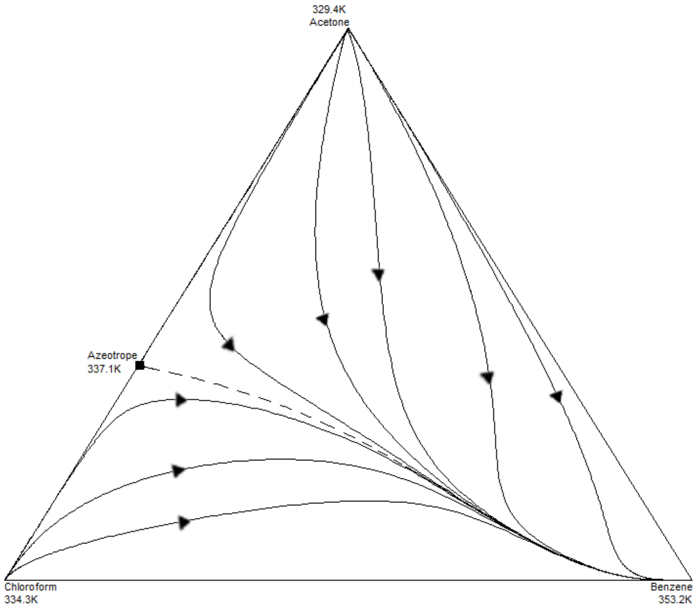

Figure 1.4. RCM of ternary system containing acetone, chloroform and benzene.

Residue curves are not to be confused with distillation lines which are smooth representations of liquid composition profiles in staged columns operating at total reflux. At infinite reflux and with an infinite number of stages, the liquid-composition trajectories in continuous distillation (as opposed to the simple batch still discussed so far) practically follow the residue curves. For a more practical column, with finite reflux and a finite number of stages, the composition profiles still exhibit the same general behavior as residue curves. Therefore, frequently the assumption that residue curves approximate the profiles in staged columns at total or finite reflux is made, because that provides a convenient tool in the preliminary steps of the design of distillation columns, either packed or staged. For instance for azeotropic separations, an RCM helps the designer to visualize feasible splits and to discard infeasible specifications. Distillation lines and boundaries can shift slightly as a function of reflux ratio and the number of stages. Wahnschafft et al (1992)[22] show where and by how much this shifting can have notable consequences in systems with simple distillation boundaries of marked curvature. Nevertheless, the error in approximating true boundaries with simple distillation boundaries in RCM's often is so small as to be inconsequential, especially at the first stage of process design.

1.4 Thesis objective and outline

Esterification processes are very interesting to be applied by reactive distillation. The synthesis of *n*-propyl propionate is one example which could be conducted in this technology. The main objective of this research is to theoretically simulate RCM's for the production of *n*-propyl propionate. These RCM's are generated using theoretical models based on thermodynamic and kinetic data for two cases: (1) non-reactive and (2) reactive.

Based on valuable data obtained by analyzing the RCM's, the feasibility of a reactive distillation concept for the production of *n*-propyl propionate is investigated. The outcome of this feasibility study predicts the possibility for substituting the conventional production route by a reactive distillation process. In literature there are already done some process design studies on the application of this technology in the production ProPro[23,24]. However, these researches are based on experimental and more extensive modeling procedures. This research could prove the usefulness of the more simple technique of RCM for the feasibility studies in reactive distillation process design.

In the second chapter of this thesis the synthesis of *n*-propyl propionate is outlined and the thermodynamic and kinetic properties of the system are described. These properties include the model for the vapor liquid equilibrium and a kinetic rate equation which are necessary for the modeling of the RCM's. The subsequent chapter shows the theoretical models for the generation of the non-reactive and reactive RCM's which shown and discussed in chapter four. Finally, conclusions are made concerning the feasibility of the reactive distillation concept for the production of *n*-propyl propionate.

Chapter 2. *n*-Propyl propionate system properties

The synthesis of *n*-propyl propionate is one of the esterification type reactions that most likely benefit from the application in a reactive distillation column. Firstly, due to the reversible character of the reaction, *in situ* withdrawal of the products makes that the equilibrium can be shifted towards the product side and that the overall conversion is increased. Furthermore, esterification reactions take place at relative low temperatures, which implies that there is an overlap between the operation window for reaction and distillation. Finally, the purification of the products in conventional processes becomes rather expensive due to the presence of multiple azeotropes in these kinds of mixtures. This can be overcome by the application of reactive distillation. In this chapter first the system and synthesis of *n*-propyl propionate is described and then the thermodynamic and kinetic properties are outlined.

2.1 *n*-Propyl propionate synthesis

n-Propyl propionate (ProPro) is a widely used solvent in automotive refinish, appliance coatings and as polymerization solvent. It is considered as a non-hazardous air pollutant by the U.S. Environmental Protection Agency which makes it a good alternative for aromatic hydrocarbon solvents like toluene and xylene[25]. Furthermore, ProPro is used as an artificial flavor in the food industry. It is synthesized by the equilibrium-limited liquid-phase esterification reaction of 1-propanol (ProOH) and propionic acid (ProAc) which is shown by equation 2.1 where k_f and k_b are the reaction rate constants for the forward and backward reaction respectively.

$$\mathrm{ProOH} + \mathrm{ProAc} \underset{k_b}{\overset{\overset{H^+}{k_f}}{\rightleftarrows}} \mathrm{ProPro} + \mathrm{water} \tag{2.1}$$

The standard enthalpy of reaction was experimentally determined to be -6.4 kJ/mol[26]. This makes that the reaction is exothermic and the chemical equilibrium constant is slightly dependent on temperature. Despite of the presence of ProAc in the reaction mixture, the reaction is not self-catalyzed and needs to be catalyzed by a strong acidic catalyst. In addition to the main esterification reaction there are also four possible side reaction that could occur[27]. Propene (Pro) is produced by the dehydration of ProOH (eq. 2.2) and the decomposition of ProPro (eq. 2.3). The formed propene could lead to the etherification of ProOH into di-n-propyl ether (ProEth) (eq. 2.4) which can also be formed by the self-condensation of ProOH (eq. 2.5). These side reactions could drastically decrease the conversion towards ProPro which is disadvantageous for the overall efficiency of the process. However, the use of Amberlyst 46 ion exchange resin to catalyze the reaction

$$\mathrm{ProOH} \xrightleftharpoons{H^+} \mathrm{Propene} + \mathrm{water} \tag{2.2}$$

$$\mathrm{ProPro} \xrightleftharpoons{H^+} \mathrm{ProAc} + \mathrm{Propene} \tag{2.3}$$

$$\mathrm{ProOH} + \mathrm{Propene} \xrightleftharpoons{H^+} \mathrm{ProEth} \tag{2.4}$$

$$2\mathrm{ProOH} \xrightleftharpoons{H^+} \mathrm{ProEth} + \mathrm{water} \tag{2.5}$$

ensures that all side reactions are suppressed[28]. This is a heterogeneous catalyst with optimal operating temperatures between 80 and 120 ^{0}C. The minimum boiling temperature of the components in the quaternary system is 97.15 ^{0}C which is that of ProOH. ProAc has the highest boiling point with 141.15 ^{0}C which shows that the operation window for reaction and distillation have an overlap at ambient pressure (1 bar).

2.2 Thermodynamics: vapor-liquid equilibrium

The quaternary system of ProPro, ProOH, ProAc and water is a highly non-ideal system both in the gas phase as in the liquid phase. Besides various azeotropes that arise, also association of highly polar substances occurs. In this phenomenon polar molecules react with each other in the vapor phase forming bi-molecules. Therefore to model the vapor-liquid equilibrium for this system, a thermodynamic model is needed that is able to account for these non-idealities. By definition at equilibrium the fugacity of one component in the vapor phase must be equal to its fugacity in the liquid phase. This way the so-called Gamma-Phi formulation of VLE can be derived by using the mathematical definitions of the fugacity's in the vapor and liquid phase[29] (eq. 2.6).

$$y_i \cdot \Phi_i(T,P,y_i) \cdot P = x_i \cdot \gamma_i(T,x_i) \cdot P_i^{sat}(T) \tag{2.6}$$

The formulation given in equation 2.6 needs correlation and thermodynamic models from which values can be obtained for the vapor pressure (P_i^{sat}), activity coefficients (γ_i) and the fugacity coefficients (ϕ_i). In equation 2.6, Φ_i is the ratio of fugacity coefficients which is defined by the expression given in equation 2.7.

$$\Phi_i = \frac{\hat{\phi}_i}{\phi_i^{sat}} \exp\left(-\frac{V_i^l (P - P_i^{sat})}{RT} \right) \tag{2.7}$$

In equation 2.7 $\phi_{\hat{i}}$ is the fugacity coefficient of species i in the vapor mixture, ϕ_i^{sat} is the fugacity coefficient of component i as a saturated vapor and V_i^l is the liquid-phase molar volume of component i. The exponential term is known as the Poynting factor and is approximately unity at low pressures which simplifies equation 2.7 to just the ratio of the fugacity coefficients.

The vapor pressure (P_i^{sat}) of the pure species is calculated by using the extended Antoine relation which is shown in equation 2.8. Here the vapor pressure is in Pascal and the temperature is in Kelvin. The Antoine coefficients are given in the pure component summary of appendix A.

$$\ln P_i^{sat} = A + \frac{B}{T} + C \cdot \ln T + D \cdot T^E \tag{2.8}$$

The activity coefficients (γ_i), which account for the non-idealities in the liquid phase, are estimated using UNIQUAC[30]. The binary interaction coefficients are given in table 2.1 and the mathematical expressions are shown in appendix B.

Table 2.1. UNIQUAC binary interaction parameters a_{ij} and b_{ij}[31]. Used as: τ_{ij}=exp(a_{ij}+ b_{ij}/T).

Component 1	*Component 2*	*a_{ij}*	*a_{ji}*	*b_{ij} [K]*	*b_{ji}[K]*
ProPro (i)	ProOH (j)	0.00	0.00	-122.7789	17.3160
ProPro (i)	ProAc (j)	0.00	0.00	-413.3753	204.9204
ProPro (i)	Water (j)	6.75	-4.47	-3212.2200	1688.5940
ProOH (i)	ProAc (j)	0.00	0.00	-281.0260	195.6222
ProOH (i)	Water (j)	1.84	-2.41	-669.0000	620.8000
ProAc (i)	Water (j)	0.00	0.00	73.800	-244.8000

The non-idealities in the vapor phase are described by the fugacity coefficients (ϕ_i) which are calculated from the virial equation of state. Since the pressure is of the system is low (1 bar) a two-term virial expansion is adequate[30] for these property calculations (eq. 2.9).

$$\frac{PV}{RT} = Z = 1 + \frac{B}{V} \tag{2.9}$$

Using the virial equation of state a relation can be obtained for the calculation of the fugacity coefficients. Introducing these expressions into equation 2.7 the following expression is found for the ratio of fugacity coefficients (Φ_i) [29] (eq. 2.10).

$$\Phi_i = \exp\left(\frac{B_{ii}(P - P_i^{sat}) + \frac{1}{2} P \sum_j \sum_k y_j y_k \left(2\delta_{ji} - \delta_{jk} \right)}{RT} \right) \tag{2.10}$$

$$\text{where,} \qquad \delta_{ji} = 2B_{ji} - B_{jj} - B_{ii}$$

$$\delta_{jk} = 2B_{jk} - B_{jj} - B_{kk}$$

The values of the virial coefficients matrix (B) are calculated using the thermodynamic model of Hayden O’Connell[32]. This model is used because of its ability to describe the phenomena of association of molecules in the vapor phase. The interaction coefficients used in this model are given in table 2.2 and the expressions for this model are given in appendix B.

Table 2.2. Hayden O'Connell association coefficients, n_{ij}^*.

Component	*ProPro*	*ProOH*	*ProAc*	*Water*
ProPro	0.00	0.00	0.00	0.00
ProOH	0.00	1.40	2.50	1.55
ProAc	0.00	2.50	4.50	2.50
Water	0.00	1.55	2.50	1.70

*** Taken from Aspen properties 2006 data bank.**

The vapor-liquid equilibrium (VLE) model (eq. 2.6) for the quaternary mixture is solved using MATLAB 2009b. Due to the non-linear character of equation 2.6 in combination with the thermodynamic models to calculate the activity coefficients, the fugacity coefficients and the vapor pressures, this equation is solved using an iterative procedure which is explained in more detail in appendix C. For a certain liquid composition and defined system pressure, the MATLAB program calculates the associated temperature and vapor composition of the vapor-liquid equilibrium. The outcome of this model is validated by comparing the model with experimental binary data[31]. All binary systems are checked so that the model is representative for all components in the quaternary system. Figure 2.1 shows the Txy- and xy-diagrams for the binary system of ProOH and ProAc. The resulting diagrams for the other binary systems are given in appendix D.

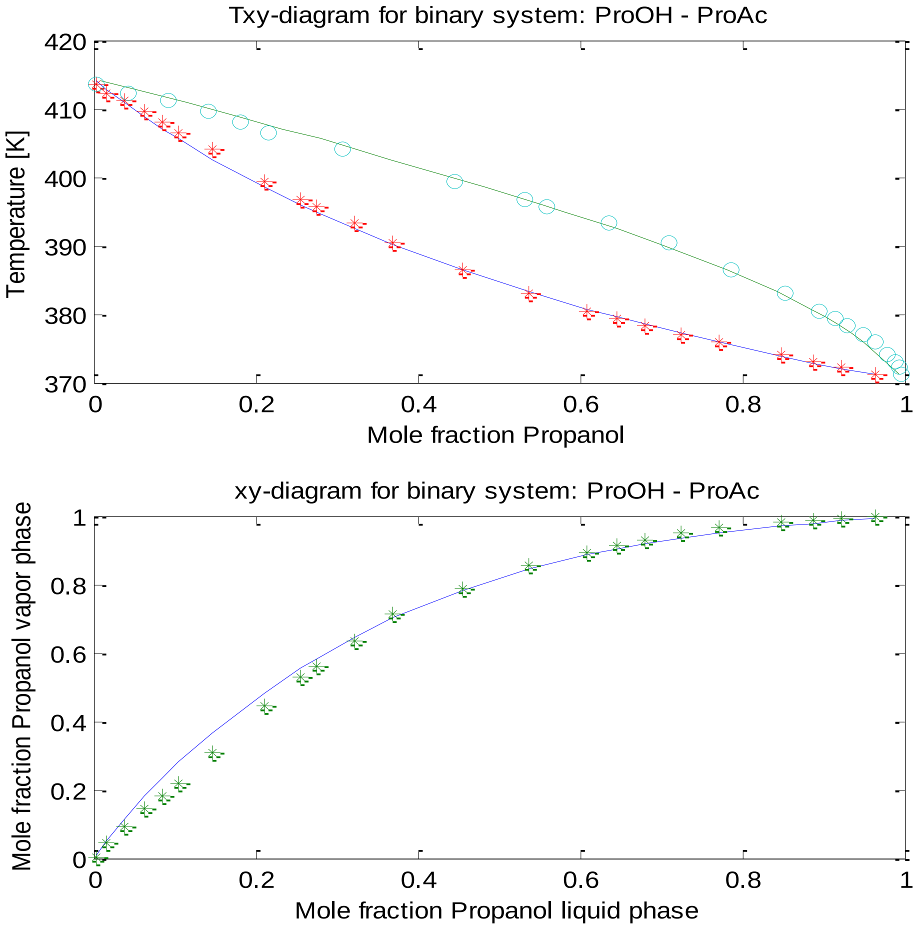

Figure 2.1. Txy- and xy-diagram for the binary system of ProOH and ProAc.

Figure 2.1 shows that for the binary system of ProOH and ProAc the model is able to predict the experimental values reasonably accurate for both the Txy- and xy-diagram. The actual goodness of all fits is determined by calculating the R^2-values for each Txy- and xy-diagram which are given in table 2.3. This table shows that for all xy-diagrams values of R^2 very close to one, which means that the vapor composition corresponding to a certain liquid composition is predicted very well. This also holds for the related temperatures except for the binary systems of water/ProPro and water/ProOH the deviation is a bit larger. Especially for the system of water and ProPro the Txy-diagram deviates from the experimental values. This is mainly caused by the highly non-ideal behavior of this binary system which is not exact described by the used model. As shown in table 2.2 the Hayden O'Connell association coefficients are not known for systems containing ProPro. In the other binary systems containing ProPro this is not significant. However, in the system water/ProPro this results in a larger error when compared with the experimental data.

Table 2.3. R^2-values for binary vapor-liquid diagrams.

Binary system:	*R^2 for Txy-diagram*	*R^2 for xy-diagram*
ProOH - ProAc	0.9981	0.9943
ProOH - ProPro	0.9881	0.9972
ProPro - ProAc	0.9908	0.9862
Water - ProPro	0.8672	0.9808
ProOH - Water	0.9454	0.9932
Water - ProAc	0.9849	0.9918

According to the literature[33], the binary systems water/ProPro, water/ProOH and water/ProAc are azeotropic systems containing a binary azeotrope. These azeotropes are also predicted by the model and these predictions and the values from literature are summarized in table 2.4. The table shows that the composition of the water/ProOH-azeotrope and the temperature of the water/ProPro-azeotrope deviate significant from the values in literature. The difference in temperature for the water/ProPro-azeotrope comes from model limitations as described above, which is also reason for the deviation of the composition for the water/ProOH azeotrope. However, the model predicts well that the water/ProOH azeotrope has the lowest temperature which is important for the topology of the distillation lines for such a system.

Table 2.4. Azeotropic data for the binary systems: water/ProPro, water/ProOH and water/ProAc.

Binary system	*Model*		*Literature*	
	Mole fraction water	Temperature [K]	Mole fraction water	Temperature[K]
Water : ProPro	0.653	360.88	0.650	363.15
Water : ProOH	0.592	360.82	0.568	360.75
Water : ProAc	0.951	372.86	0.950	373.05

2.3 Reaction kinetics

The use of Amberlyst 46 catalyst ensures that the reaction scheme for the synthesis of ProPro is only given by the esterification reaction of equation 2.1. This heterogeneous catalyzed reaction can be modeled using a pseudo-homogeneous approach since the reaction rate is not influenced by physical or chemical processes like mass transfer limitation and adsorption and desorption mechanisms. Furthermore, the heterogeneous catalyzed reaction mixture can be modeled as if it is in the presence of a homogeneous catalyst due to the fact that all active sites are located at the surface of the catalyst[34]. The rate expression for the reaction of equation 2.1 in terms of activities is given in equation 2.11.

$$r = k_f \left(a_{\text{ProOH}} a_{\text{ProAc}} - \frac{a_{\text{ProPro}} a_{\text{Water}}}{K_{eq}} \right) \tag{2.11}$$

In equation 2.11 K_{eq} is the equilibrium constant, k_f the forward reaction rate constant in [mol s^{-1} eq^{-1}] and a_i is the activity of component i. Activities are used because of the strong non-ideality of the liquid phase and these are calculated using UNIQUAC. The equilibrium constant is defined as in equation 2.12.

$$K_{eq} = \frac{k_f}{k_b} = \frac{a_{\text{ProPro}} \cdot a_{\text{water}}}{a_{\text{ProOH}} \cdot a_{\text{ProAc}}} \tag{2.12}$$

Using the kinetic rate expression, the relations of the reaction rate constant and the equilibrium constant as a function of temperature are determined by regression of experimental data. The experimental data used for this regression is generated by Duarte et al.[34] which performed kinetic batch experiments for this reaction. Therefore, to find the expressions for k_1 and K_{eq} a batch-reactor model is needed to fit these parameters to the experimental data (eq. 2.13).

$$\frac{dx_i}{dt} = \nu_i \cdot \frac{1}{N_{tot}} \cdot c_{act} m_{cat}^{dry} \cdot k_1 \left(a_{\text{ProOH}} a_{\text{ProAc}} - \frac{a_{\text{ProPro}} a_{\text{Water}}}{K_{eq}} \right) \tag{2.13}$$

In equation 2.13 ν_i is the stoichiometric coefficient of component i, N_{tot} is the total number of moles in the batch, c_{act} is the concentration of active sites on the dry catalyst and m_{cat}^{dry} is the dry catalyst mass. Duarte et al. reported that the number of active sites on the Amberlyst 46 catalyst is 0.9522 [eq kg^{-1}]. This batch-reactor model is fitted to the experimental data at three different temperatures: 353.15K, 373.15K and 388.15K. These temperatures are used because they correspond to the operating conditions of a reactive distillation process at atmospheric pressure. Using the results at these temperatures, Arrhenius-type of expressions are found for k_1 and K_{eq} which are given in equations 2.14 and 2.15 where k_1 is in [mol s^{-1} eq^{-1}].

$$K_{eq} = 7.734 \cdot 10^{-1} \exp\left(\frac{9.827 \cdot 10^{3}}{RT} \right) \tag{2.14}$$

$$k_1 = 7.060 \cdot 10^6 \exp\left(\frac{-6.652 \cdot 10^4}{RT}\right) \tag{2.15}$$

The comparison of the obtained kinetic model and the experiments is shown in figure 2.2. This figure shows the experiment at 388.15 K where the initial number of moles was 8.63 and the amount of dry catalyst mass was 5.03 grams. From the figure it can be concluded that the chemical equilibrium is predicted very well by equation 2.14 at these conditions. Also the rate of reaction (eq. 2.15) corresponds with the observed change of the mole fractions in the mixture during the experiment. This confirms that the kinetics of the heterogeneous esterification reaction can be described by a 'pseudo-homogeneous' rate equation which is formulated in activities. In appendix E the experiments at the other two temperatures are shown in comparison with the predictions of the model.

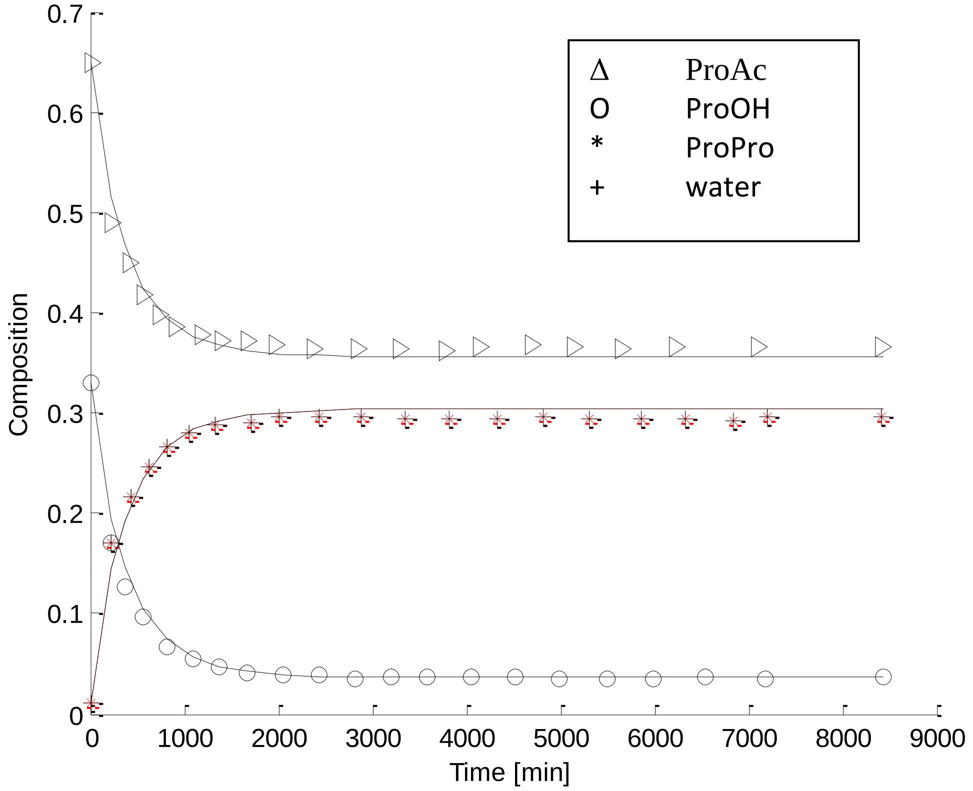

Figure 2.2. Comparison of model with experimental data at 353.15K and 10.02 gram catalyst.

Chapter 3. Mathematical model for generating RCM

As explained in the introduction, residue curve maps consist of individual residue curves which describe for a certain feed composition the dynamic behavior of the liquid phase composition along a distillation column. In case of reactive distillation processes this composition depends on the thermodynamic and kinetic properties of the system. Using the models described in the previous chapter these curves are theoretically modeled based on a single stage batch distillation experiment (figure 3.1) that corresponds to a distillation column with infinite number of stages and infinite reflux. In this chapter the theoretical models for generating RCM's are described for three different cases: (1) non-reactive RCM, (2) chemical equilibrium RCM and (3) kinetically controlled RCM. Furthermore, the mathematical determination of the singular points in the RCM is outlined.

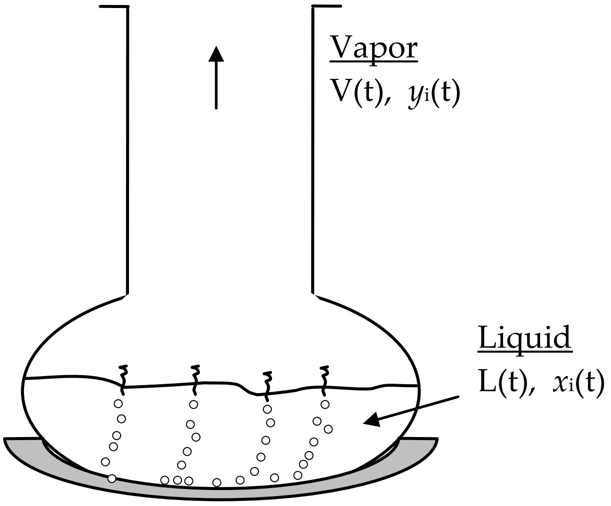

Figure 3.1. Simple batch still for the experimental determination of (non-) reactive RCM's

3.1 Non-reactive residue curve model

In the non-reactive case no reaction takes place which implies that the composition of the liquid only depends on the composition of the vapor flow leaving the still. Therefore, only a thermodynamic model is needed to describe the composition of the vapor which is in equilibrium with the liquid. The derivation of the RCM-model starts with the total mass balance (eq. 3.1) and the component mass balance (eq. 3.2) of the batch experiment shown in figure 3.1.

$$\frac{dL}{dt} = -V \tag{3.1}$$

$$\frac{dLx_i}{dt} = L\frac{dx_i}{dt} + x_i\frac{dL}{dt} = -Vy_i \tag{3.2}$$

In equation 3.1 and 3.2 L is the total moles of liquid in the batch, V is the molar vapor flow out of the still and x_i and y_i are the compositions of component i in the liquid and vapor phase respectively. Subsequently, the model can be simplified by substituting equation 3.1 into equation 3.2 and introducing a dimensionless time variable. This way the simple differential equation of equation 3.3 is obtained.

$$\frac{dx_i}{d\tau} = x_i - y_i \tag{3.3}$$

$$d\tau = \frac{V}{L}dt \tag{3.4}$$

The introduction of the dimensionless time variable τ, which is defined by equation 3.4, generalizes the model such that it is independent of the heating strategy used during the batch distillation[35, 36]. Using this model, the non-reactive RCM's can be simulated by only defining the initial liquid composition and the pressure of the system. Then the complete model for an n-component system in which no reaction takes place is given by equation 3.5, where the function $f(P,T,x_i,x_{i+1},\ldots,x_{n-1})$ indicates the model for the vapor-liquid equilibrium described in chapter 2.2.

$$\begin{aligned}
&\frac{dx_i}{d\tau} = x_i - y_i && i \in [1, n-1] \\
&y_i = f(P, T, x_i, x_{i+1}, \ldots, x_{n-1}) && i \in [1, n] \\
&\sum_{i=1}^{n} x_i = \sum_{i=1}^{n} y_i = 1 &&
\end{aligned} \tag{3.5}$$

3.2 Reactive residue curve model

The introduction of a chemical reaction into the batch distillation experiment makes that the change of the composition of the liquid is more complex. Not only the thermodynamics have to be considered, but also the kinetic effect induced by the chemical reaction. The modeling of the reactive residue curve maps can be done based on two different approaches. The first approach is to assume that the rate of reaction is infinitely fast which makes that the whole system is at chemical equilibrium at any instant in time. A second approach is to include the reaction kinetics into the RCM model to simulate the case where the process is kinetically controlled.

3.2.1 Chemical equilibrium RCM.

The equilibrium based approach assumes that when an n-component system undergoes R simultaneous chemical reactions, the reaction rate of these reactions is infinitely fast. The addition of one or more reactions to the batch distillation experiment results in the total and component molar balances of equation 3.6 and 3.7, where $\nu_{T,k}$ is the sum of the stoichiometric constants of reaction k, $\nu_{i,k}$ is the stoichiometric constant of component i in reaction k, r_k is the reaction rate of reaction k and n_{rx} is the number of simultaneous equilibrium reactions.

$$\frac{dL}{dt} = -V + \sum_{k=1}^{n_{rx}} \nu_{T,k} r_k L \tag{3.6}$$

$$\frac{dLx_i}{dt} = L\frac{dx_i}{dt} + x_i\frac{dL}{dt} = -Vy_i + \sum_{k=1}^{n_{rx}} \nu_{i,k} r_k L \tag{3.7}$$

Using the assumption of instant equilibrium, Ung and Doherty[37, 38] described a general theory for the construction of reactive RCM's based on the introduction of transformed composition variables. These variables, X_i and Y_i, are defined as shown in equation 3.8.

$$X_i = \frac{x_i - \mathbf{v}_i^T\left(\mathbf{v}_{ref}\right)^{-1}\mathbf{x}_{ref}}{1-\mathbf{v}_{total}^T\left(\mathbf{v}_{ref}\right)^{-1}\mathbf{x}_{ref}}$$

$$Y_i = \frac{y_i - \mathbf{v}_i^T\left(\mathbf{v}_{ref}\right)^{-1}\mathbf{y}_{ref}}{1-\mathbf{v}_{total}^T\left(\mathbf{v}_{ref}\right)^{-1}\mathbf{y}_{ref}} \tag{3.8}$$

In equation 3.8 $\mathbf{v}_i$ is the vector of stoichiometric coefficients for component i in all reactions n_{rx}, $\mathbf{v}_{total}$ is the vector of the total molar change for each reaction R, ref denotes the reference components for each reaction and $\mathbf{v}_{ref}$ is the square matrix of stoichiometric coefficients for the R reference components of each reaction. These transformed composition variables define a subspace of lower dimension than the normal composition variables. The characteristics of these variables are that they keep the same value for a liquid mixture before and after equilibrium is attained and that the sum of the variables is equal to one. The reference component can be either a product or a reactant, depending on the value of ν_{total}[39]. Using these transformed composition variables in equation 3.7 and substituting equation 3.6 into the equation results in the differential equation describing the reactive RCM (eq. 3.9). In equation 3.9 the dimensionless time variable τ is defined by equation 3.10 and increases monotonically with time.

$$\frac{dX_i}{d\tau} = X_i - Y_i \tag{3.9}$$

$$d\tau = \left(\frac{1-\mathbf{v}_{total}^T\left(\mathbf{v}_{ref}\right)^{-1}\mathbf{y}_{ref}}{1-\mathbf{v}_{total}^T\left(\mathbf{v}_{ref}\right)^{-1}\mathbf{x}_{ref}}\right)\cdot\frac{V}{L}\cdot dt \tag{3.10}$$

The benefit of using transformed composition variables is that the reactive RCM model (eq. 3.11) is mathematically equal to that of the non-reactive RCM (eq. 3.5), with the addition that at any instant in time the system is at chemical equilibrium.

$$\begin{aligned}
&\frac{dX_i}{d\tau} = X_i - Y_i && i \in [1, n - n_{rx} - 1] \\
&y_i = f(P, T, x_i, x_{i+1}, \dots, x_{n-1}) && i \in [1, n] \\
&K_{eq,k} = \prod_{i=1}^{i=n} (a_i)^{\nu_i} = \prod_{i=1}^{i=n} (\gamma_i x_i)^{\nu_i} && \mathrm{k} \in [1, n_{rx}] \\
&\sum_{i=1}^{n} X_i = \sum_{i=1}^{n} Y_i = 1
\end{aligned} \tag{3.11}$$

3.2.2 Kinetically controlled RCM

In cases where the rate of reaction and the rate of evaporation have the same order magnitude the operation is called kinetically controlled. This type of regime is located between the two extreme cases in which no-reaction or an infinitely fast reaction takes place. The residue curve map for this type of systems can be generated by solving the mass balances for each component in the system during the batch distillation (figure 3.1). By combining the total and components mass balance (eq. 3.6 and eq. 3.7) a differential equation can be obtained which describes the evolution of the composition in time. For an n-component mixture in which n_{rx} simultaneous reactions take place, equation 3.12 shows the expression that describes the residue curve.

$$L\frac{dx_i}{dt} = Vx_i - Vy_i + \sum_{k=1}^{n_{rx}} \nu_{i,k} r_k L - \left(\sum_{k=1}^{n_{rx}} \nu_{total,k} r_k L \right) x_i \tag{3.12}$$

In equation 3.12 $\nu_{i,k}$ is the stoichiometric constant of component i in reaction k, ν_{total} is the sum of the stoichiometric constants of reaction k and r_k is the reaction rate of reaction k. The expression for the reaction rate (r_k) is based on activities. By introducing a dimensionless time variable τ (eq. 3.4) the equation can be simplified into equation 3.13.

$$\frac{dx_i}{d\tau} = x_i - y_i + \frac{L}{V}\left[\sum_{k=1}^{n_{rx}} \nu_{i,k} r_k - \left(\sum_{k=1}^{n_{rx}} \nu_{total,k} r_k \right) x_i \right] \tag{3.13}$$

The problem in solving equation 3.13 is that the ratio L/V is not known, especially not in the first stage of the design process. This ratio depends on the size of the system and the heating strategy applied to the system. Therefore this equation cannot be solved without further specification and is not valid for the general case. This issue can be omitted by introducing the Damköhler number (Da) into equation 3.13[15, 40] which is defined by equation 3.14.

$$Da = \frac{L_0 k_{ref}}{V_0} \tag{3.14}$$

In equation 3.14, $L_{r,0}$ is the initial liquid reaction volume, V_0 is the initial vapor flow out of the still and k_{ref} is the reaction rate constant at the reference temperature which is usual chosen at the lowest boiling temperature in the mixture. The Damköhler number stands for the ratio between the characteristic times for the rate of evaporation ($L_{r,0}/V_0$) and the rate of reaction ($1/k_{ref}$). The result of introducing the Da-number into the mass balance is given by equation 3.15.

$$\frac{dx_i}{d\tau} = x_i - y_i + Da \frac{V_0}{L_0} \frac{L}{V} \frac{1}{k_{ref}} \left[\sum_{k=1}^{n_{rx}} \nu_{i,k} r_k - \left(\sum_{k=1}^{n_{rx}} \nu_{total,k} r_k \right) x_i \right] \tag{3.15}$$

By assuming an autonomous heating strategy[3.8] it can be stated that the vapor rate (V) varies in the same rate as the liquid holdup (L). This means that:

$$\frac{L}{L_0} = \frac{V}{V_0} \tag{3.16}$$

When equation 3.16 is substituted in equation 3.15 a general model is generated for the modeling of kinetically controlled RCM's with n-components, n_{rx} simultaneous chemical reactions and an autonomous heating strategy. This model is shown in equation 3.17 where k is the reaction rate constant, K_{eq} is the equilibrium constant of the reaction and a_i is the activity of component i. In order to solve this model the kinetics of all occurring reactions have to be specified. This means that all rate expressions in terms of activities have to be known and the expression for the reaction rate constants as function of the temperature have to available.

$$\begin{aligned}
&\frac{dx_i}{d\tau} = x_i - y_i + Da \frac{1}{k_{ref}} \left[\sum_{k=1}^{n_{rx}} \nu_{i,k} r_k - \left(\sum_{k=1}^{n_{rx}} \nu_{total,k} r_k \right) x_i \right] && i \in [1, n-1], k \in [1, n_{rx}] \\
&y_i = f(P, T, x_i, x_{i+1}, \ldots, x_{n-1}) && i \in [1, n] \\
&r_k = f(k, K_{eq}, a_i, a_{i+1}, \ldots, a_{n-1}) && \mathrm{k} \in [1, n_{rx}] \\
&\sum_{i=1}^{n} x_i = \sum_{i=1}^{n} y_i = 1
\end{aligned} \tag{3.17}$$

In this model the Damköhler number can be varied to generate RMC's for different reaction rates. By varying Da from 0 to ∞ the cases between no reaction and chemical equilibrium assumption can be analyzed. This way the movement of azeotropes between those cases can be modeled and the chemical equilibrium assumption can be validated for critical values of Da.

3.3 Singular point calculation in RCM's

The topology of a RCM is mainly determined by the presence of singular points in the system. These singular points correspond to non-reactive and reactive azeotropes which physically mean that the composition of the liquid does not change with time at these points. This mathematically implies that the derivative of composition with respect to time is zero for each differential equation in each considered model (3.5, 3.11 and 3.17). The temperature corresponding to these points determines the characteristics of these points in the RCM. When the temperature of a singular point is a maximum or minimum boiling point in a distillation region this point is either a stable or unstable node. Singular saddle points are characterized by having intermediate boiling points in the distillation regions. The temperature and composition of the singular points can be calculated by solving the characteristic equation for the RCM-model.

For the non-reactive case, the singular points correspond to the azeotropes in non-ideal vapor-liquid systems. At these points the compositions of the liquid and vapor phase are equal and no further separation is possible[18, 19]. The characteristic equation to locate the singular point when no reaction is occurring is given by equation 3.18.

$$0 = \mathbf{x} - \mathbf{y} \tag{3.18}$$

In equation 3.18 **x** and **y** are the composition vectors of the liquid and vapor phase respectively. The vapor composition is calculated using the appropriate model for the vapor-liquid equilibrium. In cases where the reaction does occur, also reactive azeotropes could arise where the combination between reaction and separation does not lead to a change in the liquid composition. Another effect is that singular points could disappear due to the presence of the reaction, which means that normal boiling points are overcome by the reaction. When instantaneous chemical equilibrium is assumed the characteristic equation is defined in terms of transformed variables (eq. 3.19).

$$0 = \mathbf{X} - \mathbf{Y} \tag{3.19}$$

In equation 3.19 **X** and **Y** are the transformed composition vectors defined by equation 3.8. This equation shows that for the system at chemical equilibrium the singular points are defined by having equal transformed compositions variables in each phase[42]. For the kinetically controlled regime the characteristic equation is given by equation 3.20.

$$0 = x_i - y_i + Da\frac{V_0}{L_0}\frac{L}{V}\frac{1}{k_{ref}}\left[\sum_{k=1}^{n_{rx}} \nu_{i,k} r_k - \left(\sum_{k=1}^{n_{rx}} \nu_{total,k} r_k\right) x_i\right] \qquad i \in \left[1, n-1\right], k \in \left[1, n_{rx}\right] \tag{3.20}$$

Using equation 3.20 a bifurcation analysis can be performed by solving this equation for various values of Damköhler. This way the change of the singular points from no reaction toward the chemical equilibrium assumption can be determined.

3.4 Solving methods for RCM models

The residue curve models described above for the non-reactive and reactive cases consist of various sets of nonlinear algebraic and differential equation. The entire residue curve from unstable to stable node can be obtained by integrating these models forward and backward in time starting from an initial liquid composition. The integration is done using MATLAB® version R2009b software of MathWorks. The strategy used is that the algebraic equations for the vapor-liquid equilibrium and the reaction rate are substituted into the differential equation which is numerically solved by the ode45 solver in MATLAB. This is schematically shown in appendix G. The integrator gives a numerical solution of the differential equations based on variable step size Runge-Kutta integration methods. The backward integration of the RCM models is done by transforming the models into its inverse. This way the backward integration can be done the same way as the forward integration. These backward RCM models are given in appendix F. A third input argument for the ode45 integrator, beside the mathematical model and the initial liquid composition, is the time range of the integration. This time corresponds to the dimensionless time variable τ which is defined in each model and depends on the timescale needed for the residue curve to reach its final node. In other words, this is the time needed for the batch experiment to end up in an azeotropic or pure component composition. This time depends on the initial composition of the liquid and the rate of reaction. Therefore, the timespan used to solve the RCM models varies between 5 for the equilibrium based RCM and 100 for the non-reactive RCM.

Subsequently, the residue curve maps are obtained by generating multiple residue curves at various starting composition and displaying them together in one figure. The graphical visualization of the residue curves in terms of composition variables is only possible for system containing a maximum of four components due to 3-dimensional limitations.

The characteristic equations for each model to calculate the singular points are solved by using the fsolve solver in MATLAB®. This solver uses an initial guess for the liquid composition and converges towards the composition where liquid and vapor are equal. The temperature of the singular point follows from the vapor-liquid equilibrium algorithm described in chapter 2.2. By using various initial guesses all singular point can be located.

Chapter 4. RCM's for the ProPro system

In the previous chapter models are described to theoretically generate RCM's for three different cases. In this chapter the resulting RCM's of the integration of these models are shown for the ProPro synthesis system. This is a four component system in which one reversible reaction takes place which is heterogeneously catalyzed. The topology of the maps is characterized by calculating the location and temperature of the singular points. Furthermore, a bifurcation analysis is performed to determine the influence of the reaction rate on the location of the singular points and the topology of the RCM.

4.1 Non-reactive RCM

The non-reactive RCM is obtained by solving equation 3.5 for various starting compositions of the liquid. The resulting residue curves are shown in a 3-dimensional composition space (fig. 4.1), where each vertex resembles a pure component of the system. Figure 4.1 shows that besides the pure components, the system contains five singular points. In literature only four azeotropes are described for this system[33,43], 3 binary azeotropes and one ternary azeotrope. However, the RCM shows that there is a fifth singular point in this system that is

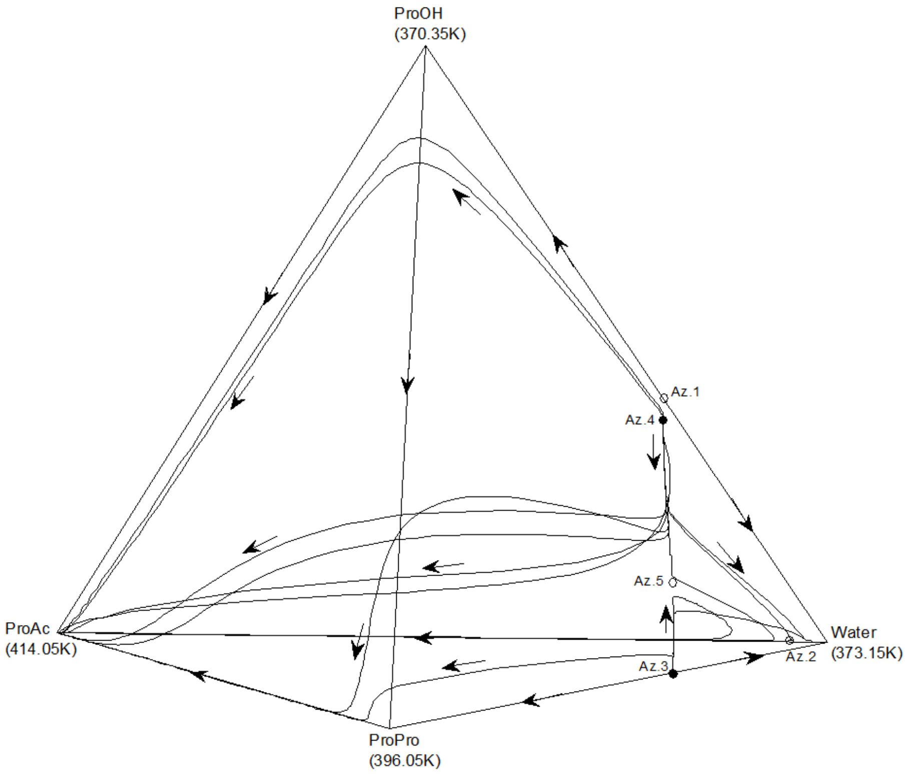

Figure 4.1. Non-reactive RCM for the quaternary system: ProOH-ProAc-ProPro-water at P = 1 bar; ● = unstable node; o = saddle point.

a solution of the characteristic equation (eq. 3.18) which holds that at this point the composition of liquid and vapor are equal at equilibrium. The nature of all singular points (pure components and azeotropes (Az.)) is determined using the procedure described by Fien and Liu[21] (see chapter 1.3). Using this terminology it can be concluded that the system contains two stable nodes, pure components ProAc and water; two unstable nodes, Az.3 and Az.4; and 5 saddle points, ProPro, ProOH, Az.1, Az.2 and Az.5. The compositions and temperatures of all azeotropes are calculated by solving equation 3.18 and this azeotropic data is resumed in table 4.1.

Table 4.1. Azeotropic data

Nr.	*Temperature [K]*	*Mole fraction*				*Type*	*Stability*
		ProOH	ProAc	ProPro	Water		
Az.1	360.82	0.408			0.592	Saddle	
Az.2	372.86		0.049		0.951	Saddle	
Az.3	360.88			0.347	0.653	Node	Unstable
Az.4	360.81	0.381		0.026	0.593	Node	Unstable
Az.5	361.05	0.108		0.249	0.643	Saddle	

Once the singular points are identified, the distillation boundaries and regions can be outlined. Since each distillation region is characterized by having one unstable node, the starting point of the residue curve, and one stable node, the end point of the residue curve, this system consists of four distillation regions. Figure 4.2 shows each possible trajectory of the curves between the nodes. The four regions are separated by two distillation boundary planes of which one is a triangle between the three binary azeotropes. This boundary plane makes that curves with certain starting compositions either end up in pure ProAc or water. The second boundary plane is a bit more difficult to visualize since it is not a flat surface. It is a curved plane that divides the composition space into an upper part where al residue curves start at Az.4 (fig. 4.2a) and a lower part where the residue curves start from Az. 3 (fig. 4.2b). Combination of these boundary planes causes the 3-dimensional composition space to be divided into four separated regions.

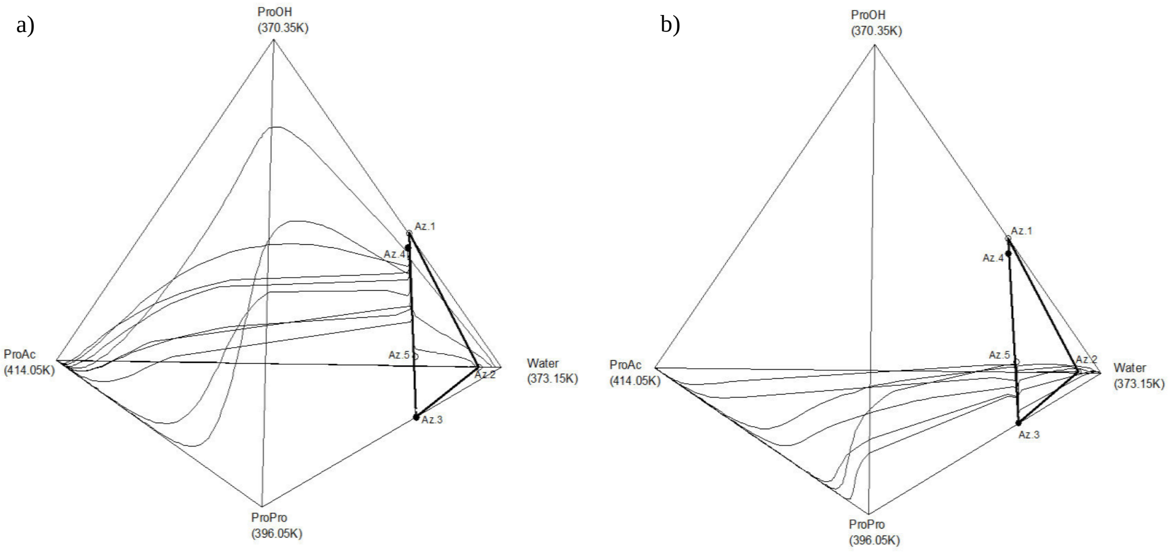

Figure 4.2. Distillation regions in non-reactive RCM for ProPro system; ● = unstable node; o = saddle point.

The presence of the fifth azeotrope explains that the residue curves either start in Az.3 or Az.4. Due to the fact that this azeotrope is not a highest or lowest boiling point in the system this singular point divides the composition space between Az.3 and Az.4 which both have lower temperatures than Az.5. Therefore such an azeotrope is also called a saddle azeotrope, which explains in this case the fact that all residue curves do not converge or diverge to this point.

4.2 Chemical equilibrium RCM

By solving equation 3.11 the reactive RCM based on the instantaneous equilibrium assumption is generated. In this simulation ProPro is chosen as the reference component to calculate the transformed compositions. The RCM in the 3-dimensional composition space (fig 4.3) shows that in presence of the reaction only two azeotropes remain in system; Az.1 and Az.2.The other azeotropes are 'reacted away' due to the reaction.

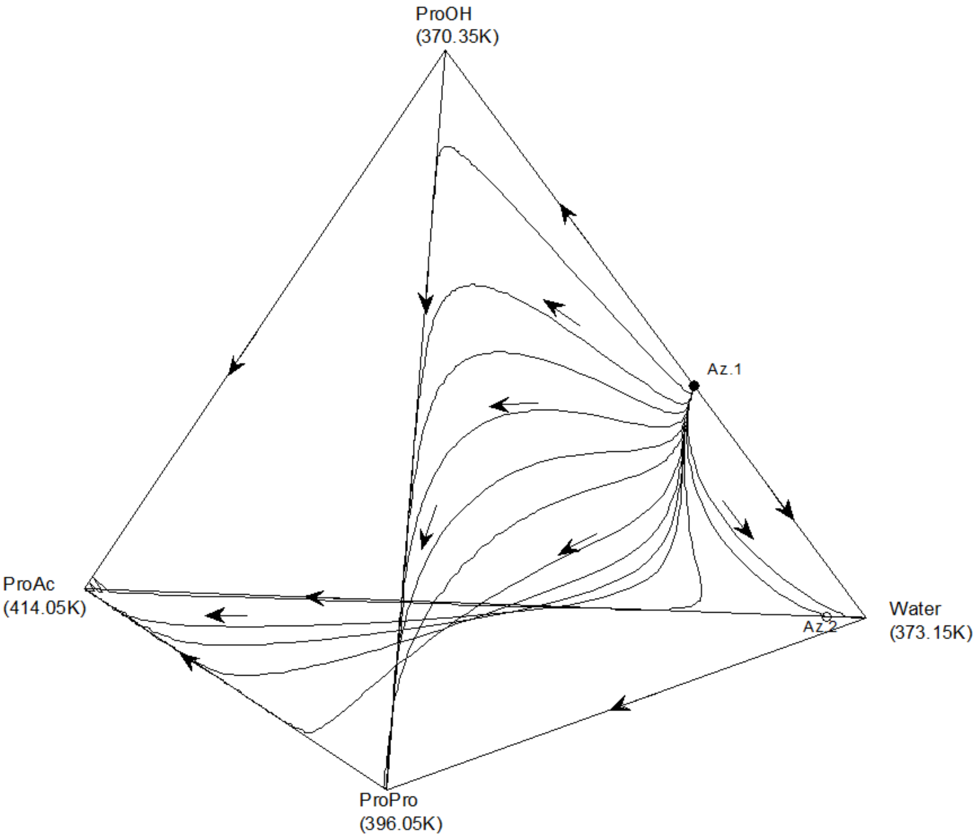

Figure 4.3. Reactive RCM for the quaternary system: ProOH-ProAc-ProPro-water at P = 1 bar.
● = unstable node; o = saddle point.

All residue curves in figure 4.3 start at the unstable node, Az.1, and depending on the starting composition they end in pure ProPro, ProAc or water. This implies that the reactive RCM contains three distillation regions in which either pure water, pure ProPro or pure ProAc can be obtained. Since pure water is only obtained when the feed contains a large mole fraction of water (>95%) this region is not of practical interest in industrial processing. The feed for industrial processing will mainly consist of a ProOH and ProAc. For these mixtures it depends on the composition of the feed which product is obtained from the reactive distillation column; ProPro or ProAc. This can be seen more clearly in figure 4.4 where the RCM is shown in a 2-dimensional plot in terms of transformed compositions. This figure shows that to obtain pure ProPro the composition of the feed should be at least 3:2 in case of feeds that only contain ProOH and ProAc.

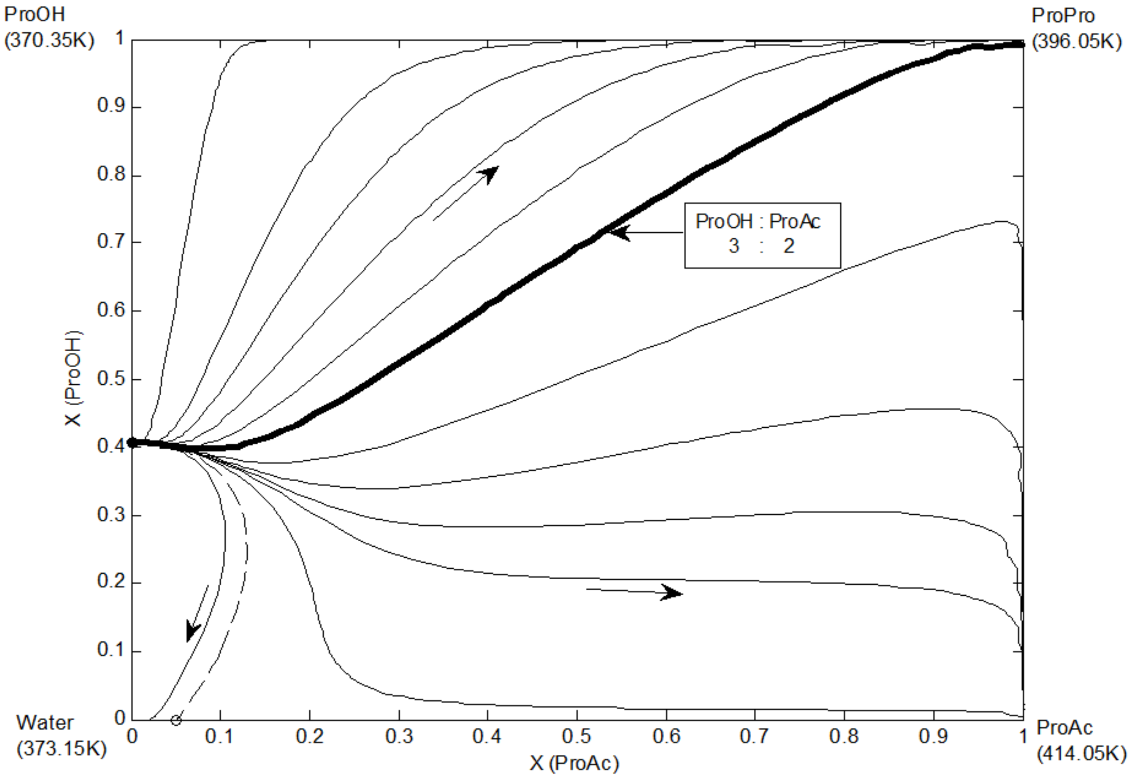

Figure 4.4. Reactive RCM in 2-dimensional transformed composition space. ● = unstable node; o = saddle point.

4.3 Kinetically controlled RCM

The transition from no reaction to equilibrium is modeled using equation 3.17 where the Damköhler number is used to model the RCM's at various ratios of reaction rate and the evaporation rate. In case of a heterogeneous catalyzed reaction, as for the synthesis of ProPro, the Damköhler number is defined as shown in equation 4.1.

$$Da = \frac{L_{r,0} m_{cat}^{dry} c_{act} k_{f,ref}}{V_0} \tag{4.1}$$

Low values of Da correspond to slow reaction rates compared to the evaporation rate while high values correspond to fast reaction rates. Since the ProPro synthesis system only contains one reaction in which the total number of moles does not change the model of equation 3.17 can be significantly simplified (eq. 4.2).

$$\begin{aligned}
&\frac{dx_i}{d\tau} = x_i - y_i + Da\frac{1}{k_{ref}}\nu_i r && i \in [1, n-1] \\
&y_i = f(P, T, x_i, x_{i+1}, \ldots, x_{n-1}) && i \in [1, n] \\
&r = k_f\left(a_{\text{ProOH}}a_{\text{ProAc}} - \frac{a_{\text{ProPro}}a_{\text{Water}}}{K_{eq}}\right) && \\
&\sum_{i=1}^{n} x_i = \sum_{i=1}^{n} y_i = 1 &&
\end{aligned} \tag{4.2}$$

The reference reaction rate constant in equation 4.2 is calculated at the boiling temperature of ProOH since this component has the lowest boiling temperature in the system. In figure 4.5 the reactive RCM's for four different values of Da are shown: Da = 0.04, 0.1,1 and 5. This figure shows that the reactive RCM changes when the reaction rate increases. At low values of Da (fig. 6a) the RCM looks most similar to the non-reactive RCM and at high values (fig. 6d) it is more similar to the equilibrium based reactive RCM. The pattern of the RCM changes

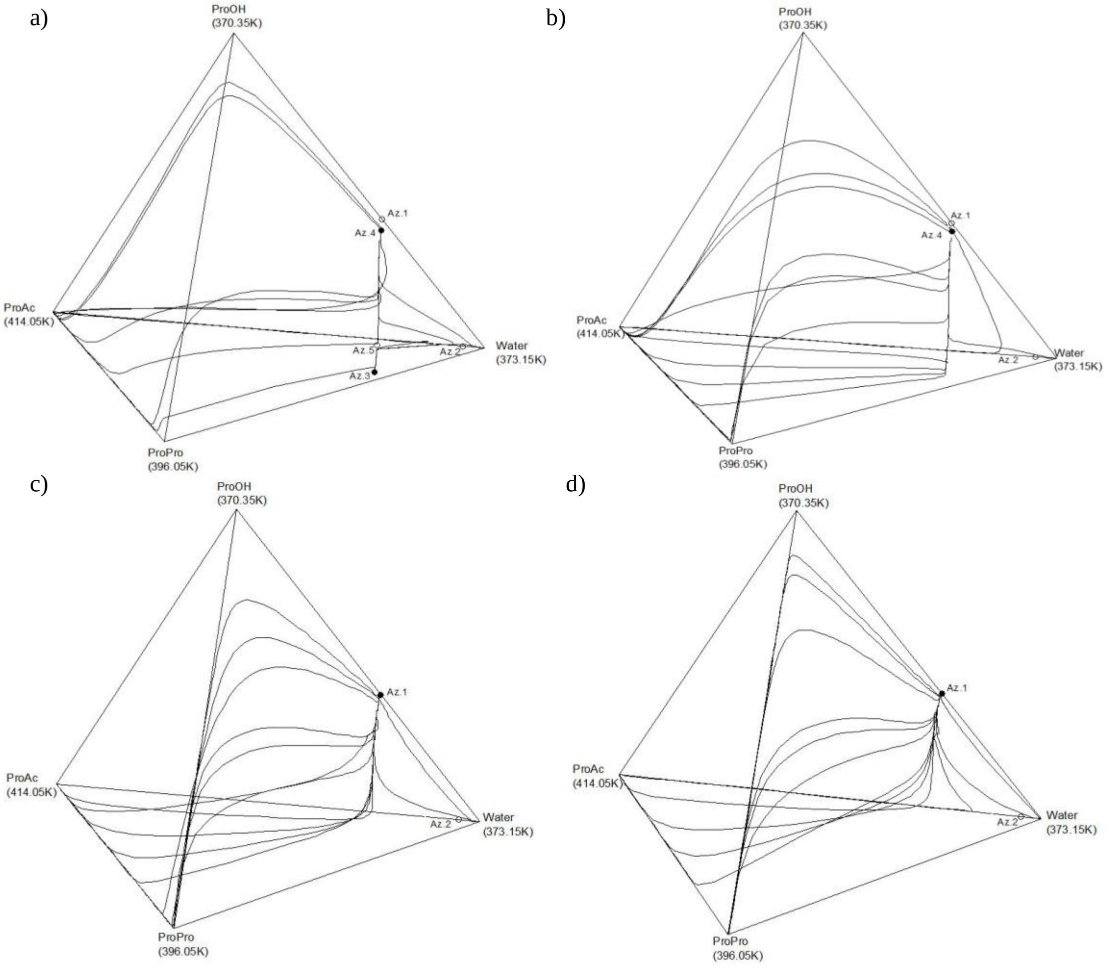

Figure 4.5. Reactive RCM for a) Da = 0.04; b) Da = 0.1; c) Da = 1; d) Da = 5.
● = unstable node; o = saddle point.

due to the fact that the singular points, e.g. the azeotropes, depend on the rate of the reaction compared to the evaporation rate (Da). At low values of Da (fig. 4.5a) all azeotropes have the same characteristics as they have in the non-reactive case and the pattern of the residue curves is still equal to the non-reactive case. However, due to the presence of the reaction the composition and the temperature of Az.3, Az.4 and Az.5 change. The temperature and composition of Az.4 changes towards that of Az.1 and azeotropes 3 and 5 move toward each other, where at Da = 0.1 (fig. 4.5b) these azeotropes have disappeared and all reside curve start at the ternary azeotrope (Az.3). When Da is further increased to 1 (fig. 4.5c), the ternary azeotrope (Az.4) has obtained the same value as azeotrope 1. This makes that the topology of this RCM is equal to the one where chemical equilibrium is assumed. At values higher than Da = 5 the RCM (fig. 4.5d) is equal to the one where chemical equilibrium is assumed.

4.4 Bifurcation analysis

The movement of the singular points as function of Da is further characterized by means of a bifurcation analysis[44]. Here the composition and temperature of the singular points is mathematically found by solving the characteristic equation (eq. 3.20). Figure 4.6 shows the bifurcation data in which the change of the five singular points is graphically shown. When there is no reaction, Da = 0, the system shows 5 singular points which are also shown in the RCM of figure 4.1. When Da increases three singular points start to move: Az.3, Az.4 and

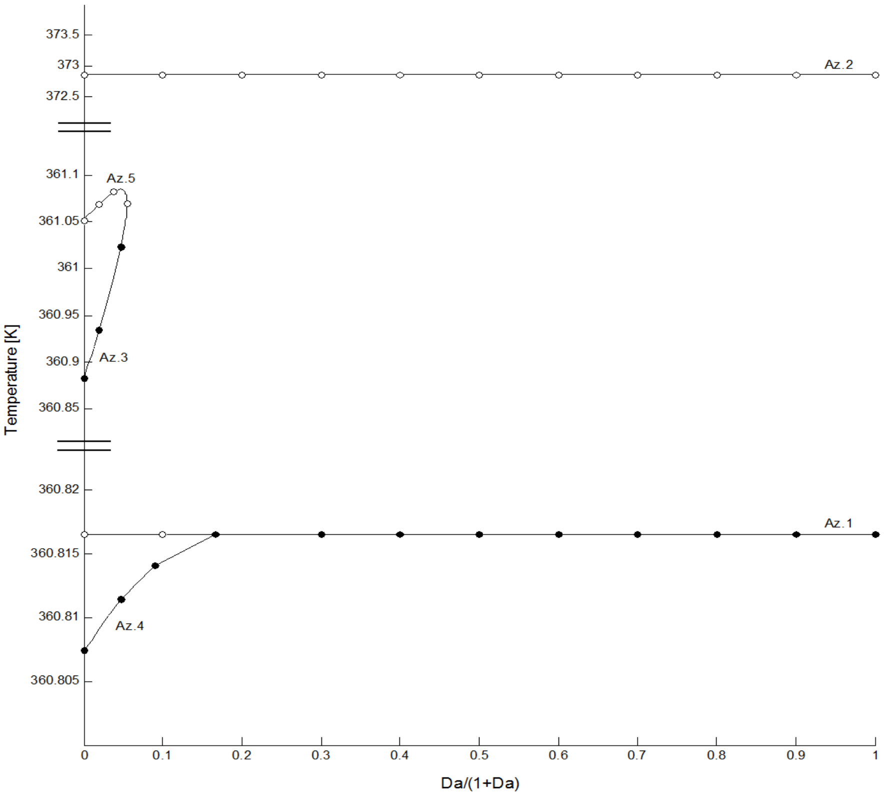

Figure 4.6. Bifurcation diagram; ● = unstable node; o = saddle point

Az.5. The other two azeotropes do not change due to a change in reaction rate. Figure 4.6 confirms the behavior seen in figure 4.5 that Az.3 and Az.5 are moving toward each other and that Az.4 moves toward Aze.2 with increasing Da. At the critical value of Da = 0.056 azeotropes 3 and 5 are equal in composition and temperature and for higher values of Da these azeotropes disappeared. For Da > 0.056 the ternary azeotrope (Az. 4) has the lowest boiling temperature in the system which makes that all residue curves start from this unstable node. When Da is increased further, Az.3 moves closer to Az.1. At a value of Da = 0.4 both azeotropes have equal temperature and composition which results in RCM's with equal characteristics as the equilibrium based RCM.

Chapter 5. Conclusions

The theoretically generated RCM's are used as a preliminary design tool for the reactive distillation concept meant for the production of ProPro. Based on these maps the feasibility of the process is assessed and a preliminary process design is deduced. As shown by the RCM's, the topology of the maps mainly depends on the rate of reaction compared to the rate of evaporation, which is reflected by the Damköhler (Da) number. At low values of Da where the reaction is slow, the RCM is characterized by five azeotropes which cause the maps to be divided into four distillation regions. With increasing reaction rate, or Da, the azeotropes change their position and temperature, and eventually azeotropes disappear, which changes the topology of the RCM. At fast reaction rates (Da > 0.4) three azeotropes are 'reacted away', leaving two binary azeotropes in the system: (1) ProOH/water and (2) ProAc/water. The consequence of this transformation between low and high values for Da is that the RCM is divided in two regions of which only one is industrially relevant. In this region the ProOH/water azeotrope is the unstable node and the stable node could be the pure component vertices of ProPro or ProAc depending on the composition of the feed. In order to obtain pure ProPro, an excess of alcohol should be used to be able to convert all ProAc. Calculations show that the minimum feed ratio of the column should be 3:2 for a two component feed of ProOH and ProAc at high values of Da. In cases where the reaction is slower this minimum ratio should be higher which means that the excess of ProOH in the feed should be larger. When no excess of ProOH is used, then a mixture of ProPro and unreacted ProAc is obtained product. Regarding the feasibility, the RCM's show that it is possible to produce ProPro by the esterification of ProOH and ProAc in a single reactive distillation column. The product is obtained at the bottom and an azeotropic mixture of ProOH and water is coming from the top of the reactive distillation column. The column can be operated at ambient pressure and the temperature should be maintained below 120^0C because of deactivation of the catalyst. Therefore, a non-reactive part should be installed at the bottom of the column to protect the catalyst from possible high temperatures in the reboiler. Another non-reactive part could be necessary in the top of the column to recover as much as possible ProPro that was distilled. Furthermore, two separate feed streams are necessary because of large boiling point differences between the reactant ProOH (T_b = 97.78 ^{o}C) and ProAc (T_b = 141.16 ^{o}C). In case of a single feed the two reactants separate directly which result in low conversion levels. Therefore, ProOH is fed at the bottom and ProAc at the top of the reactive section to induce a countercurrent flow of the reactants. Higher yield can be obtained by separating ProOH from the top product and recycling it back to the column. This separation can be done by a decanter making use of the phase split between 1-propanol and water[23], a membrane[24] or an additional distillation column.

Nomenclature

a_i = activity of component i

a_{ij}, b_{ij} = binary interaction coefficients UNIQUAC [-], [K]

B_{ii} = virial coefficient [$\mathrm{cm^3\ mol^{-1}}$]

c_{act} = concentration of active sites [$\mathrm{eq\ kg^{-1}}$]

Da = Damköhler number

k_f = forward reaction rate constant [$\mathrm{s^{-1}}$]

k_b = backward reaction rate constant [$\mathrm{s^{-1}}$]

K_{eq} = chemical equilibrium constant

L = liquid molar holdup [mol]

L_r = liquid reaction holdup [mol]

m_{cat}^{dry} = catalyst dry mass [kg]

n_c = number of components

n_r = number of reactions

n_{ij} = association coefficients Hayden O'Connell

P = pressure [bar]

P^{sat} = saturated vapor pressure [bar]

r = reaction rate [$\mathrm{mol\ s^{-1} eq^{-1}}$]

R = universal gas constant; 8.314 [$\mathrm{J\ mol^{-1}\ K^{-1}}$]

t = time [s]

T = temperature [K]

V = vapor molar flow [$\mathrm{mol\ s^{-1}}$]

V^l = liquid-phase molar volume [$\mathrm{cm^3\ mol^{-1}}$]

x_i = liquid mole fraction of species i

X_i = transformed liquid mole fraction of species i

y_i = vapor mole fraction of species i

Y_i = transformed vapor mole fraction of species i

Greek Letter

γ_i = activity of component i

ν_i = stoichiometric coefficient of species i

ν_{total} = sum of stoichiometric coefficient in a reaction

τ = dimensionless time variable, $d\tau = V/L \cdot dt$

$\hat{\phi}_i$ = fugacity coefficient of species i in gas mixture

ϕ_i^{sat} = fugacity coefficient for pure species i as saturated vapor

Φ_i = ratio of fugacity coefficients; $\Phi_i = \phi_i / \phi_i^{sat}$

Subscripts

i = component i
j = component j
k = component k
0 = Initial value
ProOH = 1-propanol
ProAc = propionic acid
ProPro = *n*-propyl propionate
ref = reference component

References

[1] IEA; World energy outlook 2011.

[2] S.Becht, R.Franke, H. Hahn, An industrial view of process intensification, *Chem.Eng.Process.* 48 (2009) 329-332.

[3] T. Van Gerven, A. Stankiewicz, Structure, energy, synergy, time - the fundamentals of Process intensification, *Ind.Eng.Chem.Res.* 48(2009) 2465-2474.

[4] A. Stankiewicz, J.A.Moulijn, Process intensification: transforming chemical engineering, *Chem.Eng.Prog.* 96 (1)(2000) 22-34.

[5] K. Sundmacher, A.Kienle, Reactive distillation, Wiley-VCH, 2003.

[6] D.L. Terrill, L.F. Sylvestre, M.F. Doherty, Separation of closely boiling mixtures by reactive distillation, *Ind.Eng.Chem.Process Des.Dev.* 24 (1985) 1062-1071.

[7] A.A. Backhaus, Continuous process for the manufacture of esters, U.S. patent 1,400,849 (1921).

[8] V.H. Agreda, High-purity methyl acetate via reactive distillation, *Chem.Eng.Prog.* 86(2)(1990) 40-46.

[9] J.A. Moulijn, M. Makkee, A. van Diepen, Chemical process technology, Wiley, 2005.

[10] W.D. Seider, J.D. Seader, D.R. Lewin, S. Wigdagdo, Product and process design principles, Wiley, 2010.

[11] C.P. Almeide-Rivera, P.L.J. Swinkels, J.Grievink, Designing reactive distillation processes: present and future, *Comp.Chem.Eng.* 38 (2004) 1997-2020.

[12] S. Giessler, R.Y. Danilov, R.Y. Pisarenko, L.A. Serafimov, S. Hasebe, I. Hashimoto, Feasibility study of reactive distillation using the analysis of the statics, *Ind.Eng.Chem.Res.* 37 (1998) 4375-4382.

[13] D.A.G. Barbosa, M.F. Doherty, The simple distillation of homogeneous reactive mixtures, *Chem.Eng.Sci.* 43 (1988) 541-550.

[14] D. Barbosa, M.F. Doherty, The influence of equilibrium chemical reactions on vapor-liquid phase diagrams, *Chem.Eng.Sci.* 43 (1988) 529-540.

[15] G. Venimadhavan, G. Buzad, Effect of kinetics on residue curve maps for reactive distillation, *AlChE.* 40, 11 (1994) 1814-1824.

[16] A. Ciric, D. Gu, Synthesis of nonequilibrium reactive distillation processes by MINLP optimization, *AIChE.* J. 40 (1994) 1479-1487.

[17] F.A.H.Z. Schreinemaker, Phys.Chem.Stoechiom.Verwandtschaftsl. 36 (1901) 257.

[18] M.F. Doherty, J.D. Perkins, On the dynamics of distillation processes III. The topological structure of ternary residue curve maps, *Chem.Eng.Sci.* 34 (1979) 1401-1414.

[19] D.B. van Dongen, M.F. Doherty, On the dynamics of distillation processes V. The topology structure of boiling temperature surface and its relation to azeotropic distillation, *Chem.Eng.Sci.* 39 (1984) 883-892.

[20] J.D. Seader, E.J. Henley, Separation process principles, Wiley, 2006.

[21] G. Fien, Y. Liu, Heuristic synthesis and shortcut design of separation processes using residue curve maps: a review, *Ind.Eng.Chem.Res.* 33 (1994) 2505-2522.

[22] O.M. Wahnschafft, J.W. Koehler, E. Blass, A.W. Westerberg, The product composition

regions of single-feed azeotropic distillation columns, *Ind.Eng.Chem.Res.* 31 (1992) 2345-2362.

[23] C. Buchaly, P.Kreis, A. Górak, Hybrid separation processes – Combination of reactive distillation with membrane separation, *Chem.Eng.Proc.* 46 (2007) 790-799.

[24] E. Altman, P. Kreis, T. van Gerven, G.D. Stefanidis, A. Stankiewicz, A. Górak, Pilot plant synthesis of n-propyl propionate via reactive distillation with decanter separator for reactant recovery. Experimental model validation and simulation studies, *Chem.Eng.Proc.* 49 (2010) 965-972.

[25] The Dow Chemical Company, October 2002b. Ucar n-propyl propionate.

[26] S.H. Ali, T. Al-Sahhaf, Synthesis of esters: Development of the rate expression for the Dowex 50 Wx8-400 catalyzed esterification of propionic acid with 1-propanol, *Chem.Eng.Sci.* 62 (2007) 3197-3217.

[27] C. Buchaly, C. Duarte, J. Loureiro, J.M. Kreis, Process intensification of n-propyl propionate synthesis using reactive distillation over a novel catalyst, ChemPor 2005.

[28] E.G. Lundquist, Catalyzed esterification process, U.S. Patent 5,426,199 (1995).

[29] J.M. Smith, H.C. van Ness, M.M. Abbott, Introduction to chemical engineering, Mc Graw-Hill, 2005, 545-568.

[30] E.B. Poling, J.M. Prausnitz, J.P. O'Connell, Properties of gases and liquids, Mc Graw-Hill, 2001.

[31] E. Altman, G.D. Stefanidis, T. van Gerven, A.I. Stankiewicz, Phase equilibria for reactive distillation of propyl propanoate. Pure component property data, vapor-liquid equilibria, and liquid-liquid equilibria, *J.Chem.Eng.Data* 56 (2011) 2322-2328.

[32] J.G. Hayden, J.P. O'Connell, A generalized method for predicting second virial coefficients, *Ind.Eng.Chem.Process Des.Dev.* 14(3) (1975) 209-216.

[33] J. Gmehling, Azeotropic data, VCH Weinheim, 1994.

[34] C. Duarte, C. Buchaly, P. Kreis, J.M. Loureiro, Esterification of propionic acid with n-propanol catalytic and non-catalytic kinetic study, *Ind.Chem.Proc.* 27 (2006) 273-286.

[35] M.F. Doherty, J.D. Perkins, On the dynamics of distillation processes I. The simple distillation of multicomponent non-reacting, homogeneous liquid mixtures, *Chem.Eng.Sci.* 33 (1978) 281-301.

[36] M.F. Doherty, J.D. Perkins, On the dynamics of distillation processes II. The simple distillation of model solutions, *Chem.Eng.Sci.* 33 (1978) 569-578.

[37] S. Ung, M.F. Doherty, Calculation of residue curve maps for mixtures with multiple equilibrium chemical reactions, *Ind.Eng.Chem.Res.* 34 (1995) 3195-3202.

[38] S. Ung, M.F. Doherty, Vapor-liquid phase equilibrium in system with multiple chemical reactions, *Chem.Eng.Sci.* 50 (1995) 23-48.

[39] S.B. Gadewar, G. Schembecker, M.F. Doherty, Selection of reference components in reaction invariants, *Chem.Eng.Sci.* 60 (2005) 7168-7171.

[40] W. Song, G. Venimadhavan, J.M. Manning, M.F. Malone, M.F. Doherty, Measurement of residue curve maps in heterogeneous kinetics in methyl acetate synthesis, *Ind.Eng.Chem.Res.* 37 (1998) 1917-1928.

[41] Y.S. Huang, K. Sundmacher, Theoretical and experimental study on residue curve maps of propyl acetate synthesis reaction, *Chem.Eng.Sci.* 60 (2005) 3363-3371.

[42] S. Ung, M.F. Doherty, Necessary and sufficient conditions for reactive azeotropes in multireaction mixtures, *AIChE.* 41 (1995) 2383-2392.

[43] S. Tlatlik, Description of n-propyl-propionate-synthesis, internal report in the frame of the EU Project "INSERT-Integrating Separation and Reaction Technologies", 2005.

[44] G. Venimadhavan, M.F. Malone, M.F. Doherty, Bifurcation study of kinetic effects in reactive distillation, *AIChE.* 45 (1999) 546-556.

Appendix

Appendix A. Pure component properties

In the table below (table A.1) the pure component properties are summarized for the quaternary system of *n*-propyl propionate, 1-propanol, propionic acid and water. Most of the properties given in the table are used in thermodynamic model to calculate the vapor-liquid equilibrium. The extended Antoine coefficients are given to calculate the vapor pressure and the volume and area parameters used in UNIQUAC. The critical properties (T_c and P_c), dipole moment and radius of gyration are used in the model of Hayden O'Connell to calculate the fugacity coefficients.

Table A.1. Pure component properties[31] of *n*-propyl propionate, 1-propanol, propionic acid and water.

		n-Propyl propionate (ProPro)	*1-Propanol (ProOH)*	*Propionic acid (ProAc)*	*Water (H_2O)*
Structure					
Molecular formula		$C_6H_{12}O_2$	C_3H_7OH	$C_3H_6O_2$	H_2O
Structural formula		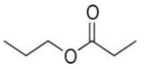	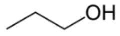	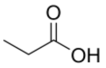	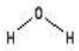
Basic properties					
Molecular weight (M_w)	[g/mol]	116.16	60.09	74.08	18.01
Boiling temperature (T_b)	[K]	350.26	351.44	373.13	391.00
Critical temperature (T_c)	[K]	568.60	536.80	600.81	647.07
Critical pressure (P_c)	[bar]	30.59	51.68	46.70	220.59
Dipole moment (μ)	[Debye]	1.7898	1.6788	1.7508	1.8492
Radius of gyration (R_g)	[Å]	4.311	2.736	3.107	0.615
Acentric factor (ω)		0.449	0.620	0.574	0.345
Antoine Parameters					
A		78.32	94.13	54.55	73.65
B		-7256.9	-8604.8	-7149.4	-7258.2
C		-8.2280	-10.1100	-432769	-7.3037
D		$4.86 \cdot 10^{-6}$	$3.13 \cdot 10^{-6}$	$1.18 \cdot 10^{-18}$	$4.17 \cdot 10^{-6}$
E		2	2	6	2
UNIQUAC					
Volume parameter (r)		4.827	2.780	2.862	0.920
Area parameter (q)		4.196	2.512	2.612	1.400

Appendix B. Thermodynamic models

In this appendix the thermodynamic models used in the calculation of the vapor-liquid equilibrium in chapter 2 are described in more detail. First, the UNIQUAC model is described and then the Hayden O'Connell model is outlined.

B.1 UNIQUAC

UNIQUAC is an activity coefficient model based on the excess Gibbs energy model described by equations B1. This excess Gibbs model consists of a combinatorial and a residual contribution. The combinatorial contribution is an entropic term quantifying the deviation from ideal solubility as a result of differences in molecule shape. The second contribution is an enthalpic correction caused by the change in interacting forces between different molecules upon mixing.

$$G^E = G^E(combinatorial) + G^E(residual)$$

$$\frac{G^E(combinatorial)}{RT} = \sum_{i=1}^{C} x_i \ln\left(\frac{\Psi_i}{x_i}\right) + \frac{Z}{2}\sum_{i=1}^{C} q_i x_i \ln\left(\frac{\theta_i}{\Psi_i}\right)$$

$$\frac{G^E(residual)}{RT} = -\sum_{i=1}^{C} q_i x_i \ln\left(\sum_{j=1}^{C} \theta_i \tau_{ij}\right)$$

$$\Psi_i = \frac{x_i r_i}{\sum_{i=1}^{C} x_i r_i}$$

$$\theta_i = \frac{x_i q_i}{\sum_{i=1}^{C} x_i q_i}$$

$$\tau_{ij} = \exp\left(\frac{u_{ji} - u_{ii}}{RT}\right) = \exp\left(a_{ij} + \frac{b_{ij}}{T}\right) \tag{B1}$$

In equation B1 the interaction coefficients a_{ij} and b_{ij} are obtained from experiments and the other variables are pure component properties: r_i, q_i (Appendix A). Using this excess Gibbs energy model the activity coefficient can be calculated using the thermodynamic definition which is given in equation B2.

$$\ln(\gamma_i) = \left(\frac{\partial\left(g^E/RT\right)}{\partial n_i}\right)_{T,P,n_{j\neq i}} \tag{B2}$$

Equation B2 shows that the activity coefficient of component i can be calculated by taking the partial derivative of the excess Gibbs energy with respect to the number of moles of this component. The result of this partial derivative is given in equation B3.

$$\ln\left(\gamma_i\right)=\ln\left(\frac{\Psi_i}{x_i}\right)+\left(\frac{Z}{2}\right)q_i\ln\left(\frac{\theta_i}{\Psi_i}\right)+l_i-\left(\frac{\Psi_i}{x_i}\right)\sum_{j=1}^{C}x_j l_j+q_i\left[1-\ln\left(\sum_{j=1}^{C}\theta_j\tau_{ji}\right)-\sum_{j=1}^{C}\left(\frac{\theta_j\tau_{ij}}{\sum_{k=1}^{C}\theta_k\tau_{kj}}\right)\right]$$

$$l_i=\left(\frac{Z}{2}\right)\left(r_i-q_i\right)-\left(r_i-1\right)$$

$$Z=10 \qquad \text{(B3)}$$

B.2 Hayden O'Connell

The model of Hayden O'Connell states that the second virial coefficient consists of several contributions:

$$B=B_{free}+B_{metastable}+B_{bound}+B_{chem} \qquad \text{(B4)}$$

In calculating B$_{\text{free}}$ a distinction can be made between nonpolar and nonpolar components. In this distinction the polar components are defined as have a dipole moment higher than 1.45 Debye. Therefore B$_{\text{free}}$ is divided into B$_{\text{free-nonpolar}}$ and B$_{\text{free-nonpolar}}$.

$$B=B_{free-nonpolar}+B_{free-polar}+B_{metastable}+B_{bound}+B_{chem} \qquad \text{(B5)}$$

The above mentioned contributions to the virial coefficient can be calculated by the following equations:

$$B_{free-nonpolar}=b_0(0.94-\frac{1.47}{T^{*'}}-\frac{0.85}{T^{*'2}}+\frac{1.015}{T^{*'3}})$$

$$B_{free-polar}=B_{free-nonpolar}-b_0\mu_{ij}^{*'}(0.75-\frac{3}{T^{*'}}+\frac{2.1}{T^{*'2}}+\frac{3}{T^{*'3}}2.1)$$

$$B_{metastable}+B_{bound}=b_0 A\exp\left(\frac{\Delta H}{kT/\varepsilon_{ij}}\right)$$

$$B_{chem}=b_0\exp\left(\eta\left[\frac{650}{\varepsilon_{ij}/k+300}-4.27\right]\right)\left(1-\exp\left(\frac{1500\eta}{T}\right)\right) \qquad \text{(B6)}$$

$$\text{for } \eta=4.5 \rightarrow \frac{650}{\varepsilon_{ij}/k+300} \text{ should be } \underset{\text{(fitted)}}{\frac{42800}{\varepsilon_{ij}/k+22400}}$$

In equation B6 the different parameters are defined as:

$$\begin{aligned}
&b_0 = \frac{2\pi}{3} N_0 \sigma_{ij}^3 \\
&T^{*'} = \left(\frac{\varepsilon_{ij}}{kT} - 1.6\omega_{ij} \right)^{-1} \\
&A = -0.3 - 0.05\mu_{ij}^* \\
&\Delta H = 1.99 + 0.2\mu_{ij}^* \\
&\mu_{ij}^{*'} = \mu_{ij}^* - 0.25 && \mu_{ij}^* \geq 0.25 \\
&\mu_{ij}^{*'} = 0 && 0.25 > \mu_{ij}^* \geq 0.04 \\
&\mu_{ij}^{*'} = \mu_{ij}^* && 0.04 > \mu_{ij}^* \geq 0
\end{aligned} \tag{B7}$$

The equations above also have several matrices containing cross coefficient between the components. The matrices are indicated by the ij-indices. These cross coefficients are calculated from the pure component parameters. The cross coefficients are defined as:

$$\begin{aligned}
&\omega_{ij} = 0.5\left(\omega_i + \omega_j\right) \\
&\sigma_{ij} = \left(\sigma_i \sigma_j\right)^{\frac{1}{2}} \\
&\varepsilon_{ij} = 0.7\left(\varepsilon_i \varepsilon_j\right)^{\frac{1}{2}} + 0.6\left(\frac{1}{\varepsilon_i} + \frac{1}{\varepsilon_j} \right)^{-1} && \text{(fitted)} \\
&\mu_{ij}^* = \frac{\mu_i \mu_j}{\varepsilon_{ij} \sigma_{ij}^3}
\end{aligned} \tag{B8}$$

The pure component parameters are calculated using the following relations:

$$\begin{aligned}
&\omega_i = 0.006R_g + 0.02087R_g^2 - 0.00136R_g^3 \\
&\sigma^{'} = \left(2.44 - \omega^{'}\right)\left(\frac{T_c}{p_c} \right)^{\frac{1}{3}} \\
&\frac{\varepsilon_i^{'}}{kT_c} = 0.748 + 0.91\omega_i - \frac{0.4\eta}{2 + 20\omega_i} \\
&\varepsilon = \varepsilon'\left(1 - \left(\frac{n}{n-6} \right)\xi\left(1 - \left(\frac{n}{n-6} + 1 \right)\frac{\xi}{2} \right) \right) \\
&\sigma^3 = \sigma'^3\left(1 + \frac{3\xi}{n-6} \right) \\
&\xi = \frac{k\mu^4}{5.723E^{-8}C\varepsilon'\sigma'^6 T_c} \\
&n = 16 + 400\omega'
\end{aligned} \tag{B9}$$

$$C = 2.882 - \frac{1.882\omega'}{0.03 + \omega'}$$

The input parameters for the Hayden O'Connell model described above are the critical temperature (T_c), pressure (P_c), dipole moment (μ), the radius of gyration (R_g) and the interaction coefficient (η). The model contains two equation which can be fitted to experimental data that are indicated in the equations B6 and B8.

Using the experimental data of Altman et al. these equations are fitted to these data for the quaternary system of *n*-propyl propionate, 1-propanol, propionic acid and water. The results are given in equations B10 and B11, where the adjusted values are indicated by a box.

$$B_{chem} = b_0 \exp\left(\eta\left[\frac{650}{\varepsilon_{ij}/k + 300} - 4.27\right]\right)\left(1 - \exp\left(\frac{1500\eta}{T}\right)\right)$$

$$\text{for } \eta = 4.5 \rightarrow \frac{650}{\varepsilon_{ij}/k + 300} \text{ should be } \frac{\boxed{33500}}{\varepsilon_{ij}/k + 22400} \qquad \text{(B10)}$$

$$\varepsilon_{ij} = \boxed{1.17957}\left(\varepsilon_i \varepsilon_j\right)^{\frac{1}{2}} + 0.6\left(\frac{1}{\varepsilon_i} + \frac{1}{\varepsilon_j}\right)^{-1} \qquad \text{(B11)}$$

Appendix C. Vapor-liquid equilibrium calculation

In chapter two the thermodynamic equilibrium is described for the non-ideal quaternary system of *n*-propyl propionate, 1-propanol, propionic acid and water. The non-linear model results in a iterative procedure to solve this, which is further explained here. The VLE-model is described by the Gamma-Phi formulation in which the extended Antoine, UNIQUAC and Hayden O'Connell are used to calculate the various coefficients (chapter 2.2). This is summarized in equation C1.

$$\begin{aligned} & y_i \Phi_i P = x_i \gamma_i P_i^{sat} \\ & P_i^{sat} = f(T) && \rightarrow \text{ Extended Antoine (eq. 2.8)} \\ & \gamma_i = f(T,x) && \rightarrow \text{UNIQUAC (Appendix B.1)} \\ & \Phi_i = f(T,P,y) && \rightarrow \text{ Hayden O'Connell (Appendix B.2)} \end{aligned} \tag{C1}$$

The model of equation C1 is highly non-linear in the unknown variables y_i and T. Therefore, this equation is solved using an iterative procedure. The algorithm of this calculation is shown in figure C1. The input for the iteration are the pressure of the system and the composition of the liquid (x_i). Using these system specifications initial guesses are estimated for the temperature (T) and the composition in the vapor phase (y_i) to start the iterative procedure. The initial guess for the temperature is calculated by the weighted average value of the saturation temperature (T_i^{sat}) of each component (eq. C2) at the pressure of the system.

$$T_{ini} = \sum_i x_i T_i^{sat} \tag{C2}$$

The values for T_i^{sat} are obtained by solving the extended Antoine equation for the temperature at the pressure of the system (eq. C3).

$$\ln P = A_i + \frac{B_i}{T_i^{sat}} + C_i \cdot \ln T + D_i \cdot \left(T_i^{sat}\right)^{E_i} \tag{C3}$$

Using the initial guess for the temperature, the values for the activity coefficients (γ_i) and the vapor pressures (P_i^{sat}) can be calculated. Then by setting all fugacity coefficients equal to one, the initial guess for the vapor composition (y_i) can be calculated by the 'Gamma-Phi' formulation (eq. C4).

$$y_i = \frac{x_i \gamma_i P_i^{sat}}{\Phi_i P} \tag{C4}$$

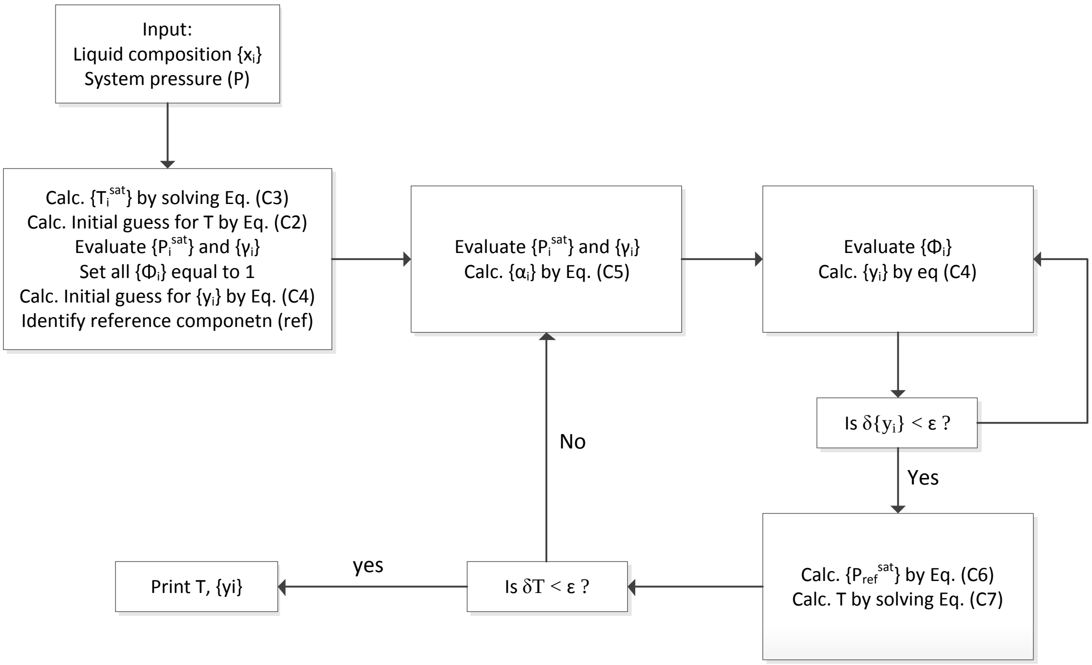

Figure C.1. Algorithm for solving the vapor-liquid equilibrium of the quaternary ProPro system.

The algorithm shown in figure C.1 contains two iterative procedures to converge to the right values of the vapor composition {y} and the temperature (T) of the vapor liquid equilibrium for given pressure and liquid composition {x}. The main structure of this procedure is that first the vapor composition is iteratively solved from the input variables and then the associated temperature is calculated making use of vapor pressure ratios (α). This temperature is compared with the input temperature and depending on the tolerance (ε) the iterative procedure is continued. Vapor pressure ratios are used because they are less sensitive to temperature in comparison with the vapor pressures, which enhances the converging of the procedure. The vapor pressure ratios are defined by equation C5.

$$\alpha_i = \frac{P_i^{sat}}{P_{ref}^{sat}} \tag{C5}$$

In equation C5, P_{ref}^{sat} is a preliminary chosen reference component at which the calculation of the temperature is based. Using the vapor pressure ratio, the updated value for the reference vapor pressure can be calculated by equation C6 which is derived from the 'Gamma-Phi formulation' (eq. C4).

$$P = \sum_i \frac{x_i \gamma_i P_i^{sat}}{\Phi_i}$$

$$P_{ref}^{sat} = \frac{P}{\sum_i \frac{y_i \gamma_i \alpha_i}{\Phi_i}} \tag{C6}$$

Subsequently, using the obtained vapor pressure the associated temperature can be calculated by solving the extended Antoine for the temperature. This equation is given by equation C7.

$$\ln P_{ref}^{sat} = A_{ref} + \frac{B_{ref}}{T} + C_{ref} \cdot \ln T + D_{ref} \cdot T^{E_{ref}} \tag{C7}$$

The outcomes of the algorithm described above are the vapor composition and system temperature at vapor-liquid equilibrium for given pressure and liquid composition. The tolerance (ε) used in the calculation has a value of $1 \cdot 10^{-6}$.

Appendix D. Comparison of VLE-model with experimental data by Txy- and xy-diagrams

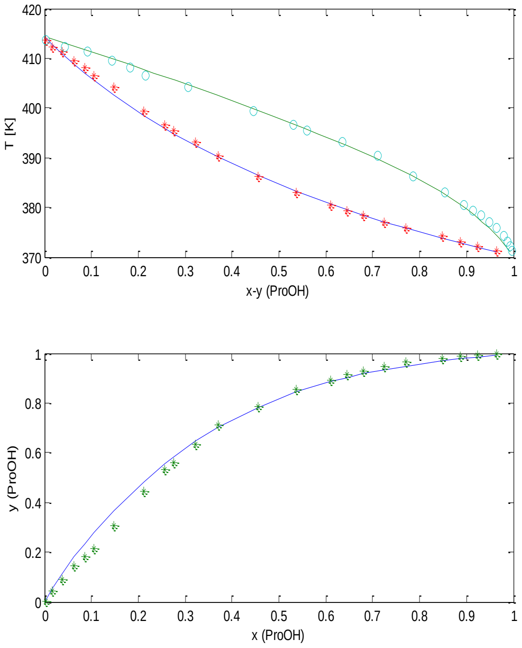

Figure D.1. 1-Propanol and propionic acid

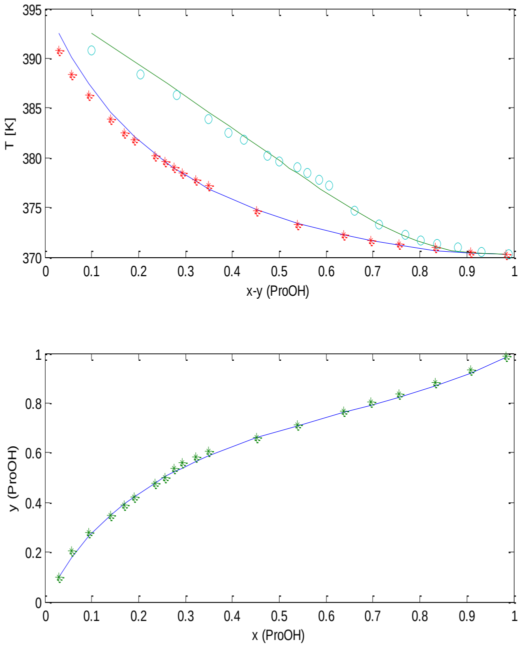

Figure D.2. 1-Propanol and *n*-propyl propionate

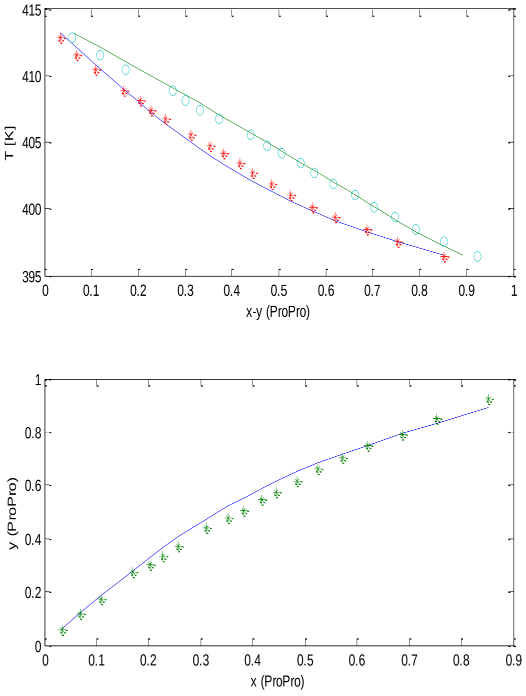

Figure D.3. *n*-Propyl propionate and propionic acid

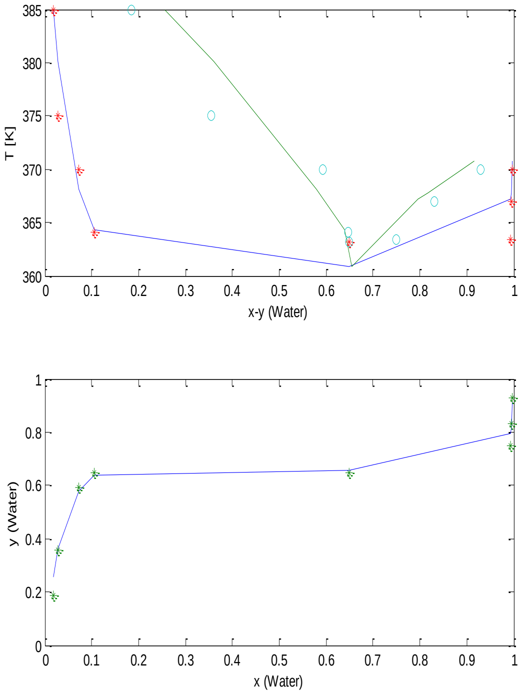

Figure D.4. Water and *n*-propyl propionate

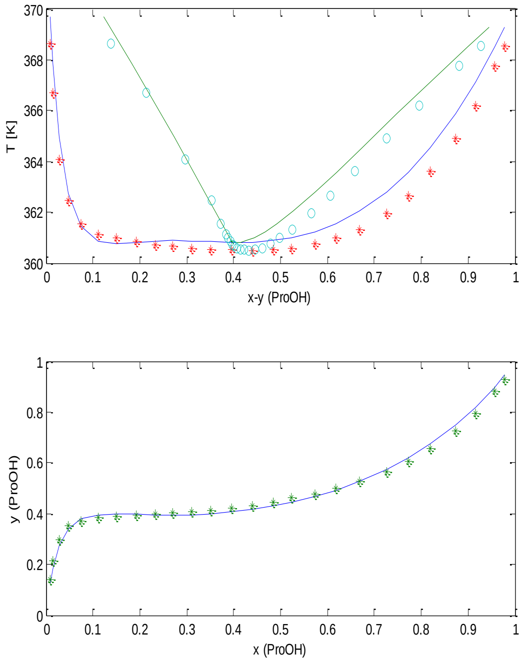

Figure D.5. 1-Propanol and water

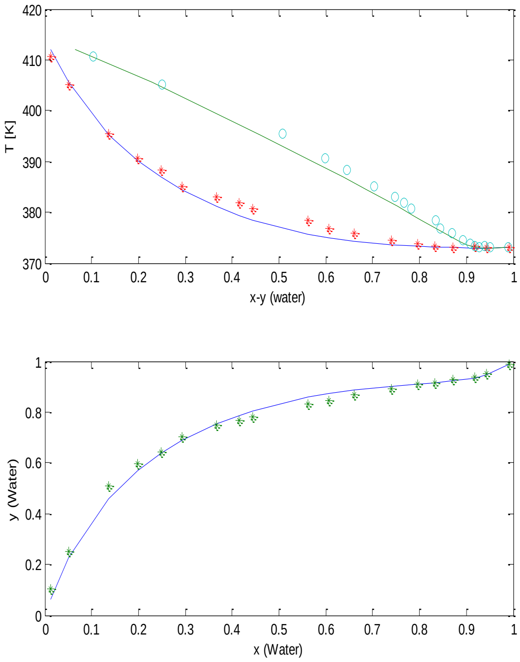

Figure D.6. Water and propionic acid

In the figures D.1 to D.6 for each binary system the Txy- and xy-diagrams are shown above each other. The upper graph shows the Txy-diagram while the lower graph shows the xy-diagrams. The axes are labeled by: x-y (i) is the composition of component i in the liquid and vapor phase; x (i) is the composition of component i in the liquid phase; y (i) is the composition of component i in the vapor phase; and T is the temperature.

Appendix E. Comparison of kinetic model with experimental data

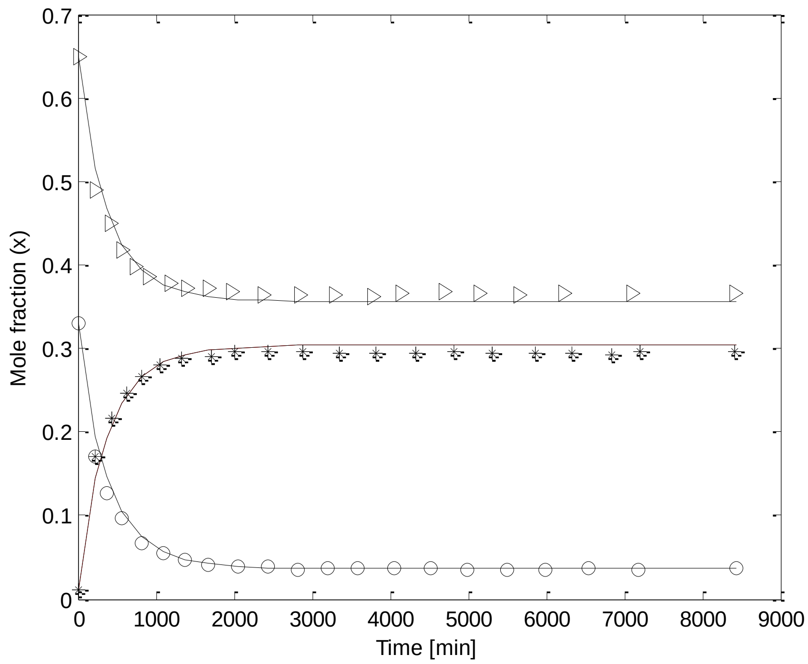

Figure E.1. Comparison of kinetic model with experimental data at 353.15K and 10.02 gram catalyst.

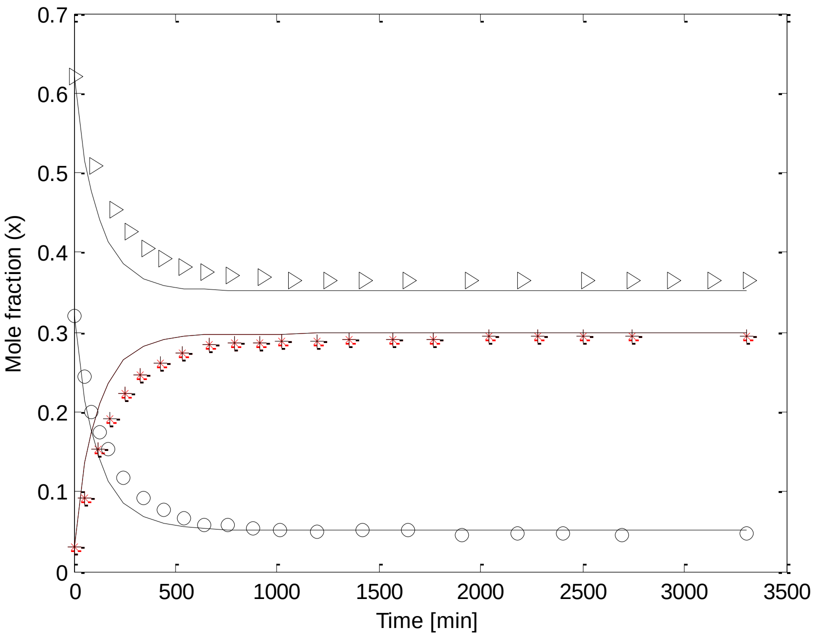

Figure E.2. Comparison of kinetic model with experimental data at 373.15K and 10.00 gramcatalyst.

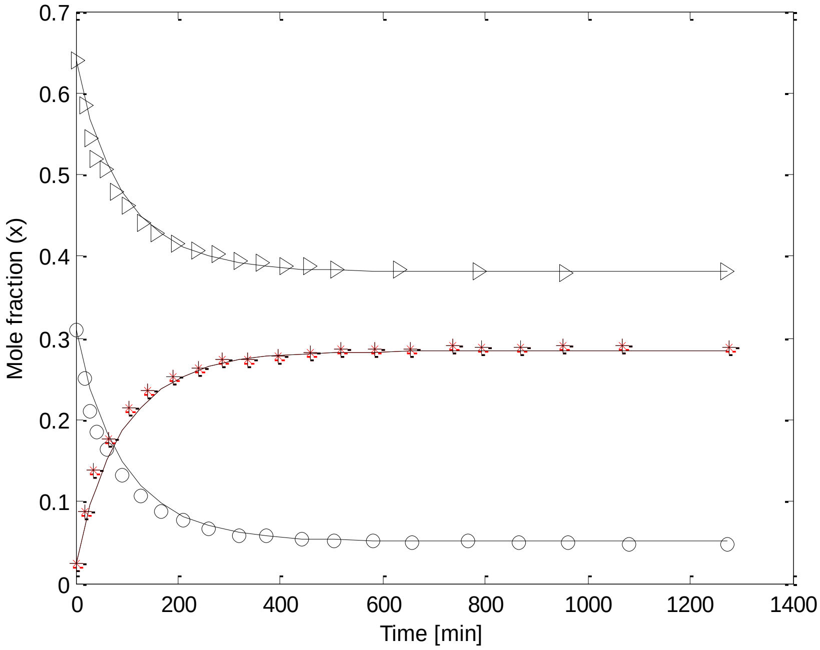

Figure E.3. Comparison of kinetic model with experimental data at 388.15K and 5.03 gram catalyst.

The figures E.1 to E.3 show the difference between the kinetic model and the experimental data for the quaternary reactive system of *n*-propyl propionate (ProPro), 1-propanol (ProOH), propionic acid (ProAc) and water. In these figures the components are marked as:

Δ = ProAc
O = ProOH
* = ProPro
\+ = Water

The solid line in the figures corresponds to the predictions of the model.

Appendix F. Models for backward RCM calculation

The generated residue curve maps in this research are obtained by integrating the described models in chapter 3 forward and backward in time. The backward integration of the models is done by transforming these models into an appropriate form in which they can be numerically solved. These backward RCM models are described below for the three different situations.

F.1 Non-reactive RCM

$$\frac{dx_i}{d\tau} = y_i - x_i \qquad i \in [1, n-1]$$

$$y_i = f(P, T, x_i, x_{i+1}, \ldots, x_{n-1}) \qquad i \in [1, n]$$

$$\sum_{i=1}^{n} x_i = \sum_{i=1}^{n} y_i = 1$$

F.2 Equilibrium RCM

$$\frac{dX_i}{d\tau} = Y_i - X_i \qquad i \in [1, n - n_{rx} - 1]$$

$$y_i = f(P, T, x_i, x_{i+1}, \ldots, x_{n-1}) \qquad i \in [1, n]$$

$$K_{eq,k} = \prod_{i=1}^{i=n} \left(a_i\right)^{\nu_i} = \prod_{i=1}^{i=n} \left(\gamma_i x_i\right)^{\nu_i} \qquad \mathrm{k} \in [1, n_{rx}]$$

$$\sum_{i=1}^{n} X_i = \sum_{i=1}^{n} Y_i = 1$$

F.3 Kinetically controlled RCM

$$\frac{dx_i}{d\tau} = y_i - x_i + Da \frac{1}{k_{ref}} \left[\sum_{k=1}^{n_{rx}} \nu_{i,k} r_k - \left(\sum_{k=1}^{n_{rx}} \nu_{total,k} r_k \right) x_i \right] \qquad i \in \left[1, n-1\right], k \in \left[1, n_{rx}\right]$$

$$y_i = f(P, T, x_i, x_{i+1}, \ldots, x_{n-1}) \qquad i \in \left[1, n\right]$$

$$r_k = f(k, K_{eq}, a_i, a_{i+1}, \ldots, a_{n-1}) \qquad \mathrm{k} \in \left[1, n_{rx}\right]$$

$$\sum_{i=1}^{n} x_i = \sum_{i=1}^{n} y_i = 1$$

Appendix G. Outline of solving the RCM models

Figure G.1 shows the structure of the MATLAB program to calculate the residue curves of the non-reactive and reactive systems. The corresponding MATLAB files are shown in the next appendix.

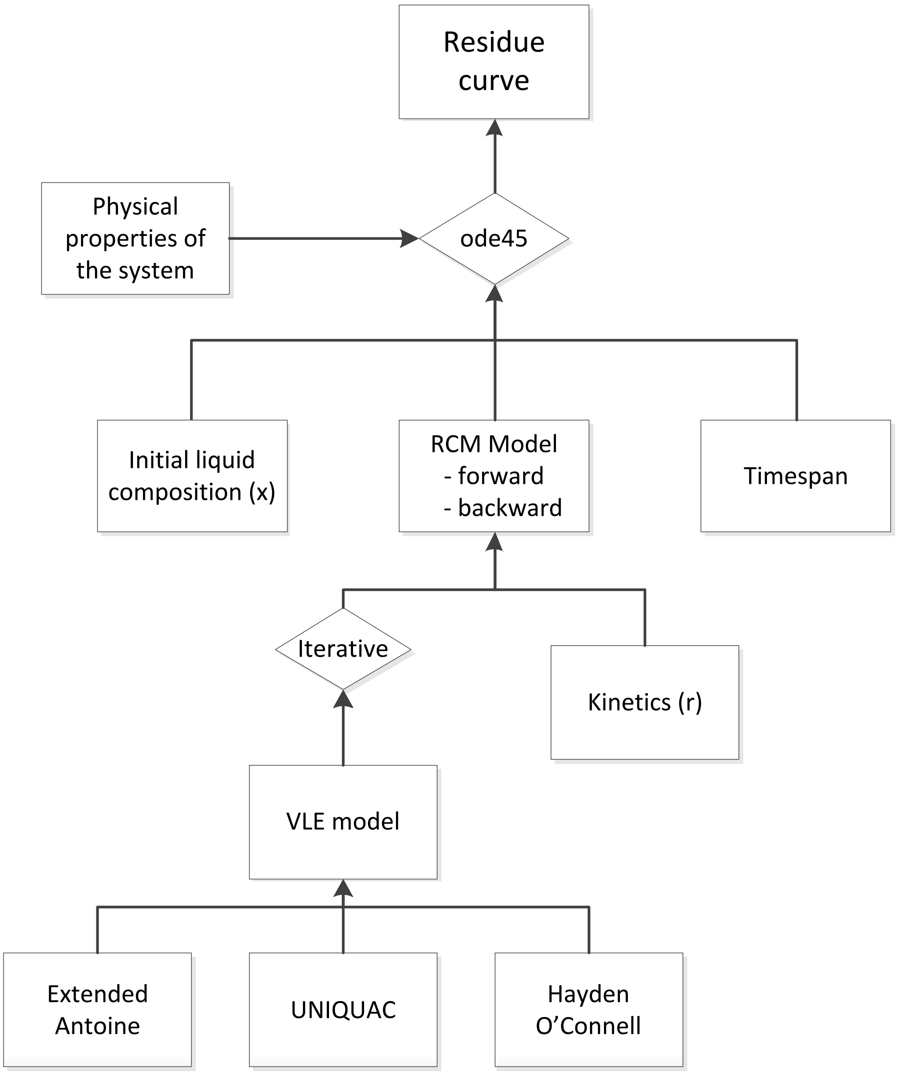

Figure G.1. Structure of the strategy to solve the RCM models.

Appendix H. MATLAB® codes

This appendix shows the MATLAB® codes that are used to generate the residue curve maps in this thesis. Therefore, it contains the thermodynamic models used in the vapor-liquid equilibrium calculation (Extended Antoine, UNIQUAC and Hayden O’Connell) and also the code where the VLE is solved. Furthermore, the codes are described from which the RCM are obtained.

H.1 Physical properties of the system

```
function [A,RP,Q,UA,UB,Properties,nij,P,R] = physical_data

% This function contains the physical properties of the species in the
% quaternary mixture needed in the written matlab codes for the generation
% of the residue curve.
% Output: Antoine coefficient matrix(A), Vector of surface parameters (Q)
%         Vector of volume parameters (RP), matrices of UNIQUAC interaction
%         coefficients (UA and UB), matrix of property row vectors
%         (Properties) containing in order: molecular weight [gram/mol],
%         boiling point [K], critical temperature [K], critical pressure
%         [bar] and volume [cm^3], dipole moment [Debye] and Radiusof
%         gyration (A), matrixof interaction parameters (nij), Pressure
%         (P) and the gas constant (R).

% Extended Antoine coefficients (P in [Pa] and T in [K])
A = [78.32  -7256.9  0  0   -8.2280  4.86e-6   2
     94.13  -8604.8  0  0  -10.1100  3.13e-6   2
     54.55  -7149.4  0  0   -4.2769  1.18e-18  6
     73.65  -7258.2  0  0   -7.3037  4.17e-6   2];


%% UNIQUAC parameters
% Volume parameters of pure components
RP = [4.82729 2.77983 2.86223 0.92];

% Area parameters of pure components
Q = [4.196 2.512 2.612 1.4];

% UNIQUAC interaction coefficients matrix A
UA = [ 0       0     0  6.75
       0       0     0  1.84
       0       0     0  0
      -4.47   -2.41  0  0   ];

% UNIQUAC interaction coefficients matrix B
UB = [   0      -122.7789  -413.3753  -3212.2200
        17.3160     0      -281.0260   -669.0000
       204.9204   195.6222     0          73.8000
      1688.5940   620.8000  -244.8000      0      ];
```

```
% Hayden O'Connell parameters
%                Mw     Tb(K)   Tc(K)   Pc(bar)   Vc(ft^3/lbmol)   mu(deby)
Properties = [ 116.16  350.26  568.60    30.59      4.5813        1.78976
                60.09  351.44  536.80    51.677     2.6911        1.67884
                74.08  373.13  600.81    46.696     0.8962        1.75079
                18.01  391.00  647.069  220.586     2.7392        1.84972

               Rd(A°)
               4.311
               2.736
               3.107
               0.615];

% Interaction coefficients
nij = [0    0      0      0
       0 1.4000 2.5000 1.5500
       0 2.5000 4.5000 2.5000
       0 1.5500 2.5000 1.7000];

%% Constants
% Pressure [bar]
P = 1.013;
% Universal Gas Constant [L bar/mol K]
R = 8.314472;
```

H.2 Extended Antoine correlation

```
function Ps = Antoine(T,A)

% This function uses the Extended Antoine correlation to calculate the
% vapor pressures for each species in an n-component system.
% Input: Temperature(T) in [K] and the Antoine coefficient matrix(A).
% Output: Vector of vapor pressures (Ps) in [bar].

[n,m] = size(A);

for i=1:n
    Ps(i)= (1e-5)*exp(A(i,1) + A(i,2)/(T+A(i,3)) + A(i,4)*T + ...
            A(i,5)*log(T) + A(i,6)*T^A(i,7));
end

Ps;
End
```

H.3 UNIQUAC

```
function GAMMA = UNIQUAC(T,Q,X,RP,UA,UB)

% This function uses the UNIQUAC model to calculate the activity
% coefficients of all components in a mixture.
% Input: Temperature(T) in [K], Vector of surface parameters (Q)
%        Vector of volume parameters (RP), Vector of liquid composition (X)
%        and matrices of UNIQUAC interaction parameters (UA and UB).
% Output: Vector of activity coefficients (GAMMA).
% Determination of number of components

NC = length(X);
```

```
% Correction for zero mole fractions to prevent dividing by zero.
for i=1:NC
    if X(i) == 0
        X(i) = 1e-14;
    end
end

% Coordination number z
z = 10;

% Calculate area fractions THETA
THETA = Q'.*X/(Q*X);
THETA;

% Calculate volume fractions PHI
PHI = RP'.*X/(RP*X);
PHI;

% Calculate l
l = 0.5*z*(RP-Q)-RP+1;
l;

% Calculate the matrix of UNIQUAC coefficients TAU
TAU = exp((UA+UB/T));
TAU;

% Calculate combinatorial part of the activity coefficients
lnGamma1 = log(PHI./X) + 0.5*z*Q'.*log(THETA./PHI)+l'-(PHI./X)*(l*X);

% Calculate residual part of the activity coefficients
for i=1:NC
    for j=1:NC
        for k=1:NC

            DENOM(k) = THETA(k)*TAU(k,j);
            DENOMSUM(j) = sum(DENOM);      % Denominater: sum of DENOM

        end

        RATIO(j) = THETA(j)*TAU(i,j)/DENOMSUM(j);
        LOG(j) = THETA(j)*TAU(j,i);

    end

    RATIOSUM(i) = sum(RATIO);
    LOGSUM(i) = sum(LOG);

    lnGamma2(i) = Q(i)*(1-log(LOGSUM(i))-RATIOSUM(i));
end

% Calculate activity coefficients
GAMMA = exp(lnGamma1+lnGamma2');

GAMMA;

end
```

H.4 Hayden O’Connell

```
function fi = HaydenOConnell(T,Y,P,Properties,nij,Ps,Theta)

% This function uses the Hayden O'connell model to calculate the ratio of
% fugacity coefficients of all species in a mixture.
% Input: Temperature (T) in [K], vector of vapor compositions (Y), Pressure
%        (P) in [bar], vector of vapor pressures (Ps) in [bar], matrix
%        of interaction parameters (nij) and matrix of property row
%        vectors (Properties) containing in order: molecular weight
%        [gram/mol], boiling point [K], critical temperature [K], critical
%        pressure [bar] and volume [cm^3], dipole moment [debye] and Radius
%        of gyration (A).
% Output: vector of fugacity coefficients ratios for each component (fi).

% Defining Hayden O'Connell parameters from Properties matrix
Tb = Properties(:,2)';                  % Boiling points
Tc = Properties(:,3)';                  % Critical temperatures
Pc = Properties(:,4)';                  % Critical Pressures
mu = Properties(:,6)';                  % Molecular dipole moment
Rd = Properties(:,7)';                  % Mean radius of gyration

% Constants
N = 6.0225e23;                          % Avogadro's number
k = 1.3805e-16;                         % Boltzmann constant [erg/K]
R = ((1.01325*22.414)/(273.15))*1000;   % Gas constant [bar*cm^3/gmol*K]


%% Pure substance parameters
% Nonpolar substances
w = 0.006026.*Rd+0.02096.*Rd.^2-0.001366.*Rd.^3;
sigmap = (2.44-w).*((Tc./(0.986923.*Pc)).^(1/3));
eps_kp = Tc.*(0.748+0.91.*w-0.4.*diag(nij)'./(2+(20.*w)));

% Polar, nonassociating substances mu > 1.45
n = 16+400.*w;
C = 2.882-1.882.*w./(0.03+w);

for i=1:length(Tc)              % Loop over each component

     if mu(i)<1.45                % If mu < 1.45 , not affected  by polarity
        Xi(i) = 0;              % Xi is zero
        eps(i) = eps_kp(i)*k;
        sigma(i) = sigmap(i);
     else

        Xi(i) = mu(i)^4/(5.723e-8*C(i)*eps_kp(i)*(sigmap(i)^6)*Tc(i));
     % If mu > 1.45 , influence of
     % polarity, calculation of Xi
        eps(i) = eps_kp(i)*k*(1-(n(i)/(n(i)-6))*Xi(i)*...
                  (1-((n(i)/(n(i)-6))+1)*0.5*Xi(i)));
        sigma(i) = (sigmap(i)^3*(1+3*Xi(i)/(n(i)-6)))^(1/3);
     end
end

Xi;
eps;
sigma;

%% Calculation of cross coefficients
```

```
for i=1:length(Tc)
     for j=1:length(Tc)
         wij(i,j)=0.5*(w(i)+w(j));
         sigmaijp(i,j) = (sigma(i)*sigma(j))^0.5;
         epsijp(i,j) = 1.17957*(eps(i)*eps(j))^0.5+...
                        0.6*((1/eps(i)+1/eps(j))^-1);
         muij(i,j) = (1e-18)^2*mu(i)*mu(j)/(epsijp(i,j)*...
                      (sigmaijp(i,j)*1e-8)^3);

        % Account for the effect of induction for polar(i)-nonpolar(j)
        % systems when mu(i)>2.0
        if mu(i)>=2 & mu(j)==0
             Xiij(i,j) = ((mu(i)^2)*(eik(j)^(2/3))*(sigmai(j)^4))/...
                          (eijkp(i,j)*(sigmaijp(i,j)^6));
        elseif mu(i)==0 & mu(j)>=2
             Xiij(i,j) = ((mu(j)^2)*(eik(i)^(2/3))*(sigmai(i)^4))/...
                          (eijkp(i,j)*(sigmaijp(i,j)^6));
        else
             Xiij(i,j) = 0;
        end
     end
end

wij;
sigmaijp;
epsijp;
muij;

c1p = (16+(400.*wij))./(10+(400.*wij));    % Redefinition of c1 using w(i,j)
c2p = 3./(10+(400.*wij));                  % Redefinition of c2 using w(i,j)
sigmaij = sigmaijp.*((1-(Xiij.*c2p)).^(1/3));
epsij = epsijp.*(1+(Xiij.*c1p));

sigmaij;
epsij;

for i=1:length(Tc)
     for j=1:length(Tc)
         b0ij(i,j) = (2/3)*pi*N*((sigmaij(i,j)*1e-8)^3); % b0ij [cm^3/gmol]
         Aij(i,j) = -0.3-0.05*muij(i,j);                  % Aij
         dHij(i,j) = 1.99+0.2*muij(i,j)^2;
         Tstar(i,j) = (epsij(i,j)/(k*T)-1.6*wij(i,j))^-1;

       if muij(i,j)<0.04
             muijp(i,j) = muij(i,j);
       elseif 0.04<=muij(i,j)<0.25
             muijp(i,j) = 0;
       else
             muijp(i,j) = muij(i,j)-0.25;
       end

       if nij(i,j)<4.5
             C1(i,j) = 650/(epsij(i,j)/k+300);
       else
             C1(i,j) = 34170/(epsij(i,j)/k+22400);
       end

         B_nonpolar(i,j) = b0ij(i,j)*(0.94-1.47/Tstar(i,j)-...
                           0.85/Tstar(i,j)^2+1.015/Tstar(i,j)^3);
         B_polar(i,j) = b0ij(i,j)*muijp(i,j)*(0.75-3/Tstar(i,j)+...
```

```
                         2.1/Tstar(i,j)^2+2.1/Tstar(i,j)^3);
         B_free(i,j) = B_nonpolar(i,j)-B_polar(i,j);
         B_metastablebound(i,j) = b0ij(i,j)*Aij(i,j)*exp(dHij(i,j)/...
                                  (k*T/epsij(i,j)));
         B_chem(i,j) = b0ij(i,j)*exp(nij(i,j)*(C1(i,j)-4.27))*...
                        (1-exp(1500*nij(i,j)/T));
         Bij(i,j) = B_nonpolar(i,j)+B_polar(i,j)+B_metastablebound(i,j)+...
                     B_chem(i,j);
     end
end

muijp;
b0ij;
Aij;
dHij;
Tstar;
B_nonpolar;
B_polar;
B_metastablebound;
B_chem;
Bij;


%% Calculation of fugacity coefficients and there ratio
for k=1:length(Tc)
     for i=1:length(Tc)
         for j=1:length(Tc)

              deltaik = 2*Bij(i,k)-Bij(i,i)-Bij(k,k);
              deltaij = 2*Bij(i,j)-Bij(i,i)-Bij(j,j);

              SUMFUN(j) = Y(i)*Y(j)*(2*deltaik-deltaij);
         end

         SUM(i)=sum(SUMFUN);
     end
    DSUM(k) = sum(SUM);

    fip(k) = exp((P/(R*T))*(Bij(k,k)+0.5*DSUM(k)));
    fis(k) = exp(Bij(k,k)*Ps(k)/(R*T));

end

fip;
fis;

fi = fip./fis;
```

H.5 Vapor-liquid equilibrium

```
function[Y T] = vapor_comp(X)

% This function calculates the vapor-liquid equilibrium for the
% quaternary system containing n-propyl propionate, 1-propanol,
% propionic acid and water. It uses the Gamma-Phi formulation where the
% activity coefficients are calculated using UNIQUAC, the vapor pressures
% with the extended Antoine correlation and the fugacity coefficients
% with the method of Hayden O'Connell.
% Input: vector of liquid compositions (X)
% Uses: physical_data, Saturated_T, UNIQUAC, Antoine, Hayden_O’Connell
% output: Vapor composition (Y) and Temperature (T) of VLE

[A,RP,Q,UA,UB,Properties,nij,P,R] = physical_data;

Ts = Saturated_T(P,A);
T_ini = Ts*X;
Ps_ini = Antoine(T_ini,A);
GAMMA_ini = UNIQUAC(T_ini,Q,X,RP,UA,UB);
Alpha_ki_ini = Ps_ini./Ps_ini(1);
fi_ini = [1 1 1 1];
Y_ini = Ps_ini'.*X.*GAMMA_ini./(fi_ini'.*P);

tol = 1e-6;              % Tolerance

Y = Y_ini;               % Initial guess Y
T = T_ini;               % Initial guess T

for j=1:100

    Ps = Antoine(T,A);
    GAMMA = UNIQUAC(T,Q,X,RP,UA,UB);
    Alpha_ki = Ps./Ps(1);

    for i=1:100

        tel = i;

        fi = HaydenOConnell(T,Y,P,Properties,nij,Ps);
        Y_new = Ps'.*X.*GAMMA./(fi'.*P);
        Y_new = Y_new./sum(Y_new);

        dY = abs(Y-Y_new);

     if dY<tol
     break

     else Y = Y_new;
     end

    end

    Ps_j = P./sum(X.*Alpha_ki'.*(GAMMA./fi'));

    Ts = Saturated_T(Ps_j,A);
    T_new = Ts(1);

    dT = abs(T-T_new);
```

```
if dT<tol
break

else T = T_new;
end

end

Y = Y';
T;

============================================================================

function Ts = Saturated_T(P,A)

% This function uses the Extended Antoine correlation to calculate the
% saturated temperature of each component at a specified pressure.
% Input: Pressure (P) in [K] and the Antoine coefficient matrix(A).
% Output: Vector of saturated temperatures (Ts) in [K].


[n,m] = size(A);

%Antoine coefficient matrix for initial guess calculation
B = [7.20119  1501.07  224.94
     7.77374  1518.16  213.076
     7.66944  1727.17  219.512
     8.05573  1723.64  233.076];

% Solving Ts using fsolve from the extended Antoine correlation
for i=1:n

    Ts0(i) = B(i,2)/(B(i,1)-log10(P/0.00133))-B(i,3)+273.15;

    options = optimset('MaxIter',100000,'TolX', 1e-6,
              'MaxFunEvals',100000);

    [Ts(i)] = fsolve(@fun_Ts,Ts0(i),options,A,P,i);

end

Ts;

end


      function f = fun_Ts(Ts,A,P,i)

      f = ((1e-5)*exp(A(i,1) + A(i,2)/(Ts+A(i,3)) + A(i,4)*Ts +...
           A(i,5)*log(Ts) + A(i,6)*Ts^A(i,7)))-P;
      end
```

H.6 Non-reactive RCM

```
clc
clear all
close all

%% System
comp1 = 'n-Propyl propionate';
comp2 = '1-Propanol';
comp3 = 'Propionic acid';
comp4 = 'Water';

[A,RP,Q,UA,UB,Properties,nij,P,R] = physical_data;

%% Initial liquid compositions in mole fractions
Data = [0.40    0.30    0.02
        0.20    0.20    0.05
        0.05    0.30    0.02
        0.05    0.10    0.02
        0.05    0.70    0.02
        0.05    0.05    0.05
        0.85    0.05    0.05
        0.05    0.85    0.05
        0.05    0.05    0.85
        0.35    0.10    0.10
        0.15    0.05    0.05
        0.15    0.05    0.01];

%% Calculating the residue curves for each initial liquid composition

[m,n] = size(Data);

for i = 1:m

    % Mole fractions
    X1 = Data(i,1);
    X2 = Data(i,2);
    X3 = Data(i,3);

    % Vector of liquid compositions
    X_0 = [X1;X2;X3;1-X1-X2-X3];

    %% Solving the differential equation
    % Calculating the forward RC
    tauspan = linspace (0,10);

    [tau,X] = ode45(@(tau,X)
              fun_nonreactRCM_for(tau,X,A,RP,Q,UA,UB,Properties,nij,P,R),ta
              uspan,X_0);

    Xf = X;

    [p,q] = size(Xf);

    Xf_end(i,:) = Xf(p,:);



    % Calculating the backward RC
```

```
tauspan = linspace (0,50);

[tau,X] = ode45(@(tau,X)
          fun_nonreactRCM_back(tau,X,A,RP,Q,UA,UB,Properties,nij,P,R),t
          auspan,X_0);
Xb = X;

[p,q] = size(Xb);

Xb_end(i,:) = Xb(p,:);


%% plot in 3-dimension composition space
% 3D plot

xaf = Xf(:,1);
xbf = Xf(:,4);
xcf = Xf(:,3);
xdf = Xf(:,2);
XXf = xbf+0.5*xcf+0.5*xdf;
YYf = 0.5*sqrt(3)*xcf+1/6*sqrt(3)*xdf;
ZZf = sqrt(2/3)*xdf;

xab = Xb(:,1);
xbb = Xb(:,4);
xcb = Xb(:,3);
xdb = Xb(:,2);
XXb = xbb+0.5*xcb+0.5*xdb;
YYb = 0.5*sqrt(3)*xcb+1/6*sqrt(3)*xdb;
ZZb = sqrt(2/3)*xdb;

XX(:,i) = [XXf; XXb];
YY(:,i) = [YYf; YYb];
ZZ(:,i) = [ZZf; ZZb];

AA = [0 0 0];
BB = [1 0 0];
CC = [0.5 0.5*sqrt(3) 0];
DD = [0.5 (1/6)*sqrt(3) sqrt(2/3)];
allx = [AA(1) BB(1) DD(1) AA(1) CC(1) DD(1) BB(1) CC(1)];
ally = [AA(2) BB(2) DD(2) AA(2) CC(2) DD(2) BB(2) CC(2)];
allz = [AA(3) BB(3) DD(3) AA(3) CC(3) DD(3) BB(3) CC(3)];


figure(2)
plot3(XXf, YYf, ZZf, '-k')
hold on
plot3(XXb, YYb, ZZb,'-k')

axis square
xlim([0 1])
ylim([0 1])
zlim([0 1])
line(allx, ally, allz);

sp = 0.05;
text(AA(1)-sp,AA(2)-sp,AA(3)-sp, 'ProPro');
text(BB(1)+sp,BB(2)-sp,BB(3)-sp, 'Water');
text(CC(1)-sp,CC(2)-sp,CC(3)-sp, 'ProAc');
```

```
    text(DD(1),DD(2),DD(3)+sp, 'ProOH');

    grid off
end

===========================================================================

function dXdtau =fun_nonreactRCM_for(tau,X,A,RP,Q,UA,UB,Properties,nij,P,R)

% This function describes the forward path of the RCM. It uses the liquid
% composition vector and calculates the VLE of the system at this
% composition.
% Returns the differential equation of the forward path of the RCM. It
% describes the change of the liquid composition in time.

for i=1:4
    if X(i) < 0.00001;
        X(i)=0;
    end
end

X = X./sum(X);

% Calculation of the vapor composition in equilibrium with the liquid
Y = vapor_comp(X,A,RP,Q,UA,UB,Properties,nij,P,R);

% Differential equation describing the forward liquid composition in time
dXdtau = X-Y';

end

===========================================================================

function dXdtau=fun_nonreactRCM_back(tau,X,A,RP,Q,UA,UB,Properties,nij,P,R)

% This function describes the backward path of the RCM. It uses the liquid
% composition vector and calculates the VLE of the system at this
% composition.
% Returns the differential equation of the backward path of the RCM. It
% describes the change of the liquid composition in time.

for i=1:4
    if X(i) < 0.0001;
        X(i)=0;
    end
end

X = X./sum(X);

% Calculation of the vapor composition in equilibrium with the liquid
Y = vapor_comp(X,A,RP,Q,UA,UB,Properties,nij,P,R);

% Differential equation describing the backward liquid composition in time
dXdtau = Y'-X;

end
```

H.7 Chemical equilibrium RCM

```
clc
clear all
close all

%% System
comp1 = 'n-Propyl propionate';
comp2 = '1-Propanol';
comp3 = 'Propionic acid';
comp4 = 'Water';

%% Properties of the system
[A,RP,Q,UA,UB,Properties,nij,P,R] = physical_data;

%% Kinetic parameters
nu = [1 -1 -1 1];
ref = 1;
Comp = [2 3 4];

%% Initial transformed liquid compositions
Data = [0.60 0.39];
        0.05 0.05
        0.10 0.10
        0.20 0.20
        0.20 0.79
        0.30 0.69
        0.40 0.59
        0.50 0.49
        0.60 0.39
        0.65 0.34
        0.70 0.29
        0.75 0.24
        0.80 0.19
        0.90 0.09];

[m,n] = size(Data);

for i = 1:m

    % Mole fractions
    XT1 = Data(i,1);
    XT2 = Data(i,2);

    % Vector of liquid compositions
    XT_0 = [XT1 XT2];

    %% Solving the differential equation for the reactive RCM

    % Calculating the forward RC
    tauspan = linspace (0,5);

    [tau,XT] = ode45(@(tau,XT)
               fun_reactRCM_for(tau,XT,A,RP,Q,UA,UB,Properties,nij,P,R,nu,r
               ef,Comp),tauspan,XT_0);

    XTf = [XT(:,1) XT(:,2) 1-XT(:,1)-XT(:,2)];
```

```
for j=1:100
    XT = [XTf(j,1); XTf(j,2); 1-XTf(j,1)-XTf(j,2)];

    % Initial guess for the reference composition
    Xref_0 = min(XT(1),XT(2));

    % Using fsolve to calculate the Xref
    options = optimset('MaxIter',100000,'TolX', 1e-6,
              'MaxFunEvals',100000);
    Xref = fsolve(@(Xref)
           solve_Xref(Xref,XT,A,RP,Q,UA,UB,Properties,nij,P,R,nu,ref,Co
           mp),Xref_0,options);

    if Xref > 1
        Xref = 1;
    end

    X = Xrecalc(XT,nu,Xref,ref,Comp);

    for k=1:4
       if X(k) < 0.000000001;
             X(k) = 0;
       end
    end

    X = X./sum(X);

    Xt = X';
    Xf(j,:) = Xt;
    Xr(j,1) = Xref;
end

[p,q] = size(Xf);

Xf_end(i,:) = Xf(p,:)

% Calculating the backward RC
tauspan = linspace (0,30);

[tau,XT] = ode45(@(tau,XT)
           fun_reactRCM_back(tau,XT,A,RP,Q,UA,UB,Properties,nij,P,R,nu,
           ref,Comp),tauspan,XT_0);

XTb = [XT(:,1) XT(:,2) 1-XT(:,1)-XT(:,2)];

for j=1:100

    XT = [XTb(j,1); XTb(j,2); 1-XTb(j,1)-XTb(j,2)];

    % Initial guess for the reference composition
    Xref_0 = min(XT(1),XT(2));

    % Using fsolve to calculate the Xref
    options = optimset('MaxIter',100000,'TolX', 1e-6,
              'MaxFunEvals',100000);
    Xref = fsolve(@(Xref)
           solve_Xref(Xref,XT,A,RP,Q,UA,UB,Properties,nij,P,R,nu,ref,Co
           mp),Xref_0,options);
```

```
    if Xref > 1
        Xref = 1;
    end
    X = Xrecalc(XT,nu,Xref,ref,Comp);

    for k=1:4
        if X(k) < 0.000000001;
             X(k) = 0;
        end
    end

    X = X./sum(X);

    Xt = X';
    Xb(j,:) = Xt;
    Xr(j,1) = Xref;
end

[p,q] = size(Xb);

Xb_end(i,:) = Xb(p,:)

%% plot in 3-dimensional composition space
xaf = Xf(:,1);
xbf = Xf(:,4);
xcf = Xf(:,3);
xdf = Xf(:,2);
XXf = xbf+0.5*xcf+0.5*xdf;
YYf = 0.5*sqrt(3)*xcf+1/6*sqrt(3)*xdf;
ZZf = sqrt(2/3)*xdf;

xab = Xb(:,1);
xbb = Xb(:,4);
xcb = Xb(:,3);
xdb = Xb(:,2);
XXb = xbb+0.5*xcb+0.5*xdb;
YYb = 0.5*sqrt(3)*xcb+1/6*sqrt(3)*xdb;
ZZb = sqrt(2/3)*xdb;

XX(:,i) = [XXf; XXb];
YY(:,i) = [YYf; YYb];
ZZ(:,i) = [ZZf; ZZb];

AA = [0 0 0];
BB = [1 0 0];
CC = [0.5 0.5*sqrt(3) 0];
DD = [0.5 (1/6)*sqrt(3) sqrt(2/3)];
allx = [AA(1) BB(1) DD(1) AA(1) CC(1) DD(1) BB(1) CC(1)];
ally = [AA(2) BB(2) DD(2) AA(2) CC(2) DD(2) BB(2) CC(2)];
allz = [AA(3) BB(3) DD(3) AA(3) CC(3) DD(3) BB(3) CC(3)];

figure(2)
plot3(XXf, YYf, ZZf,'-k')
hold on
plot3(XXb, YYb, ZZb,'-k')
hold on

axis square
xlim([0 1])
ylim([0 1])
```

```
    zlim([0 1])
    hold on
    line(allx, ally, allz);
    sp = 0.05;
    text(AA(1)-sp,AA(2)-sp,AA(3)-sp, 'ProPro');
    text(BB(1)+sp,BB(2)-sp,BB(3)-sp, 'Water');
    text(CC(1)+sp,CC(2)+sp,CC(3)-sp, 'ProAc');
    text(DD(1),DD(2),DD(3)+sp, 'ProOH');
    grid off

    % 2D plot of transformed variables
    figure(3)
    plot(XTf(:,2),XTf(:,1),'-k',XTb(:,2),XTb(:,1),'-k')
    hold on
    sp = 0.02;
    text(1+sp,1, 'ProPro');
    text(0-0.10,0, 'Water');
    text(1+sp,0, 'ProAc');
    text(0-0.10,1, 'ProOH');
    axis([0 1 0 1])
end

===========================================================================

function [dXTdtau Xref_for] =
                              fun_reactRCM_for(tau,XT,A,RP,Q,UA,UB,Propertie
                              s,nij,P,R,nu,ref,Comp)

% This function describes the forward path of the reactive RCM. It uses
% the liquid transformed composition vector (XT) and the solved value for
% Xref from 'solve_Xref' to calculate the VLE of the system at
% this composition and the equilibrium constant.
% Returns the differential equation of the forward path of the reactive
% RCM in terms of transformed variables. It describes the change of the
% liquid composition in time.

XT = [XT(1); XT(2); 1-XT(1)-XT(2)];

% Initial guess for the reference composition
Xref_0 = min(XT(1),XT(2));

% Using fsolve to calculate the Xref
options = optimset('MaxIter',100000,'TolX', 1e-6, 'MaxFunEvals',100000);

Xref = fsolve(@(Xref)
       solve_Xref(Xref,XT,A,RP,Q,UA,UB,Properties,nij,P,R,nu,ref,Comp),Xref
       _0,options);

X = Xrecalc(XT,nu,Xref,ref,Comp);

for i=1:4
   if X(i) < 0.000000001;
         X(i) = 0;
   end
end
X = X./sum(X);

[Y T] = vapor_comp(X,A,RP,Q,UA,UB,Properties,nij,P,R);
Keq = fun_Keq(X,T,Q,RP,UA,UB);
```

```
Y = Y';

YT = Ytrans(Y,nu,ref);

XT = [XT(1); XT(2)];
YT = [YT(1); YT(2)];

dXTdtau = XT-YT;
end

===========================================================================

function dXTdtau = 
                   fun_reactRCM_back(tau,XT,A,RP,Q,UA,UB,Properties,nij,P,R
                   ,nu,ref,Comp)

% This function describes the backward path of the reactive RCM. It uses
% the liquid transformed composition vector (XT) and the solved value for
% Xref from 'solve_Xref' to calculate the VLE of the system at
% this composition and the equilibrium constant.
% Returns the differential equation of the backward path of the reactive
% RCM in terms of transformed variables. It describes the change of the
% liquid composition in time.

XT = [XT(1); XT(2); 1-XT(1)-XT(2)];

% Initial guess for the reference composition
Xref_0 = min(XT(1),XT(2));

% Using fsolve to calculate the Xref
options = optimset('MaxIter',100000,'TolX', 1e-6, 'MaxFunEvals',100000);

Xref = fsolve(@(Xref)
       solve_Xref(Xref,XT,A,RP,Q,UA,UB,Properties,nij,P,R,nu,ref,Comp),Xref
       _0,options);

Xref;

X = Xrecalc(XT,nu,Xref,ref,Comp);

for i=1:4
    if X(i) < 0.000000001;
         X(i) = 0;
    end
end

X = X./sum(X);

[Y T] = vapor_comp(X,A,RP,Q,UA,UB,Properties,nij,P,R);

Keq = fun_Keq(X,T,Q,RP,UA,UB);

Y = Y';

YT = Ytrans(Y,nu,ref);

XT = [XT(1); XT(2)];
YT = [YT(1); YT(2)];
```

```
dXTdtau = YT-XT;
end

===========================================================================

function Keq = fun_Keq(X,T,Q,RP,UA,UB)

% This function calculates the value of the chemical equilibrium constant
% based on activity. Therefore it uses the temperature (T), the composition
% of the reaction mixture (X) and the activity coefficients (GAMMA).
% This function return the equilibrium constant (Keq)

GAMMA = UNIQUAC(T,Q,X,RP,UA,UB);
ACT = GAMMA.*X;

Keq = ACT(1)*ACT(4)/(ACT(2)*ACT(3));
end

===========================================================================

function F =solve_Xref(Xref,XT,A,RP,Q,UA,UB,Properties,nij,P,R,nu,ref,Comp)

% This function describes the calculation of the value for Xref at which
% both the vapor-liquid equilibrium and the chemical equilibrium hold. It
% uses the transformed composition vector (XT) and function to calculate
% the VLE and Keq.
% It returns the minimization function for solving with a solver.

X = Xrecalc(XT,nu,Xref,ref,Comp);

for i=1:4
    if X(i) < 0.000001;
         X(i) = 0.000001;
    end
end

X = X./sum(X);

% Function calculating the VLE
[Y T] = vapor_comp(X,A,RP,Q,UA,UB,Properties,nij,P,R);

% Function calculating the chemical equilibrium constant
Keq = fun_Keq(X,T,Q,RP,UA,UB);

F = abs(Keq-0.7734*exp(9827/(R*T)));
end



============================================================================



function X = Xrecalc(XT,nu,Xref,ref,Comp)

% Determining the number of components(NC) and number of reaction(NR)
[NR,~] = size(nu);
```

```
NC = length(XT)+NR;
m = length(XT);
X = zeros(NC,1);

% Sum of the stoichiometric coefficients, total molar change and building
the square matrix of stoichiometric coefficients for the
% reference components in the each reaction


for i=1:NR

    nu_T(i) = sum(nu(i,:));

    for j = 1:NR

        nu_ref(i,j) = nu(i,ref(j));

    end
end

% Elimate the reference component from the stoichiometric matrix
for i=NR:-1:1

    nu(:,ref(i)) = [];
end

x = XT+(nu*inv(nu_ref)*Xref')'

for i=1:m
    X(Comp(i)) = x(i);
end

for i=1:NR
    X(ref(i)) = Xref(i);
end

X;
end

============================================================================

function XT = Xtrans(X,nu,ref)

% Determining the number of components(NC) and number of reactions(NR)
NC = length(X);
[NR,~] = size(nu);

% Isolating the reference component and eliminating it from  the X vector
Xref = X(ref);
X(ref) = [];

% Sum of the stoichiometric coefficients, total molar change and building
the square matrix of stoichiometric coefficients for the
% reference components in the each reaction
for i=1:NR
    nu_T(i) = sum(nu(i,:));

    for j = 1:NR
```

```
        nu_ref(i,j) = nu(i,ref(j));
    end
end

% Elimate the reference component from the stoichiometric matrix
for i=NR:-1:1

    nu(:,ref(i)) = [];
end

% Calulating the transformed variable for the liquid composition: XT
XT = (X-nu'*inv(nu_ref)*Xref);

XT;
end

===========================================================================

function YT = Ytrans(Y,nu,ref)

% Determining the number of components(NC) and number of reaction(NR)
NC = length(Y);
[NR,~] = size(nu);

% Isolating the reference component and eliminating it from  the X vector
Yref = Y(ref);
Y(ref) = [];

% Sum of the stoichiometric coefficients, total molar change and building
the square matrix of stoichiometric coefficients for the
% reference components in the each reaction
for i=1:NR

    nu_T(i) = sum(nu(i,:));

    for j = 1:NR

        nu_ref(i,j) = nu(i,ref(j));

    end
end

% Elimate the reference component from the stoichiometric matrix
for i=NR:-1:1

    nu(:,ref(i)) = [];
end

% Calulating the transformed variable for the liquid composition: XT
YT = (Y-nu'*inv(nu_ref)*Yref);
YT;
end
```

H.8 Kinetically controlled RCM

```
clc
clear all
close all

%% System
comp1 = 'n-Propyl propionate';
comp2 = '1-Propanol';
comp3 = 'Propionic acid';
comp4 = 'Water';

%% Properties of the system
[A,RP,Q,UA,UB,Properties,nij,P,R] = physical_data;

%% System specification
Da = 0.05;
nu = [1 -1 -1 1];
ref = 1;

%% Initial liquid compositions in mole fractions
Data = [0.34    0.01    0.01
        0.40    0.30    0.02
        0.20    0.20    0.05
        0.05    0.30    0.02
        0.05    0.10    0.02
        0.05    0.70    0.02
        0.05    0.05    0.05
        0.85    0.05    0.05
        0.05    0.85    0.05
        0.05    0.05    0.85
        0.35    0.10    0.10
        0.15    0.05    0.05
        0.15    0.05    0.01];

[m,n] = size(Data);

for i = 1:m

    % Mole fractions
    X1 = Data(i,1);
    X2 = Data(i,2);
    X3 = Data(i,3);

    % Vector of liquid compositions
    X_0 = [X1;X2;X3;1-X1-X2-X3];

    %% Solving the differential equation for kinetically controlled RCM
    % Calculating the forward RCM
    tauspan = linspace (0,10);

    [tau,X] = ode45(@(tau,X)
              fun_kineticRCM_for(tau,X,A,RP,Q,UA,UB,Properties,nij,P,R,Da,n
              u),tauspan,X_0);

    [p,q] = size(Xf);

    Xf_end(i,:) = Xf(p,:);
    % Calculating the backward RCM
```

```
tauspan = linspace (0,75);

[tau,X] = ode45(@(tau,X)
          fun_kineticRCM_back(tau,X,A,RP,Q,UA,UB,Properties,nij,P,R,Da,
          nu),tauspan,X_0);
[p,q] = size(Xb);

Xb_end(i,:) = Xb(p,:);

%% plot in 3-dimensional composition space
xaf = Xf(:,1);
xbf = Xf(:,4);
xcf = Xf(:,3);
xdf = Xf(:,2);
XXf = xbf+0.5*xcf+0.5*xdf;
YYf = 0.5*sqrt(3)*xcf+1/6*sqrt(3)*xdf;
ZZf = sqrt(2/3)*xdf;

xab = Xb(:,1);
xbb = Xb(:,4);
xcb = Xb(:,3);
xdb = Xb(:,2);
XXb = xbb+0.5*xcb+0.5*xdb;
YYb = 0.5*sqrt(3)*xcb+1/6*sqrt(3)*xdb;
ZZb = sqrt(2/3)*xdb;

XX(:,i) = [XXf; XXb];
YY(:,i) = [YYf; YYb];
ZZ(:,i) = [ZZf; ZZb];

AA = [0 0 0];
BB = [1 0 0];
CC = [0.5 0.5*sqrt(3) 0];
DD = [0.5 (1/6)*sqrt(3) sqrt(2/3)];
allx = [AA(1) BB(1) DD(1) AA(1) CC(1) DD(1) BB(1) CC(1)];
ally = [AA(2) BB(2) DD(2) AA(2) CC(2) DD(2) BB(2) CC(2)];
allz = [AA(3) BB(3) DD(3) AA(3) CC(3) DD(3) BB(3) CC(3)];

figure(2)
plot3(XXf, YYf, ZZf, '-r')
hold on
plot3(XXb, YYb, ZZb,'-b')

axis square
xlim([0 1])
ylim([0 1])
zlim([0 1])
line(allx, ally, allz);

sp = 0.05;
text(AA(1)-sp,AA(2)-sp,AA(3)-sp, 'ProPro');
text(BB(1)+sp,BB(2)-sp,BB(3)-sp, 'Water');
text(CC(1)-sp,CC(2)-sp,CC(3)-sp, 'ProAc');
text(DD(1),DD(2),DD(3)+sp, 'ProOH');

xlabel('x1');
ylabel('x2');
ylabel('x3');
grid off
```

```
    % Plot in transformed variables
    XTf = Xtrans(Xf,nu,ref);
    XTb = Xtrans(Xb,nu,ref);

    % 2D plot of transformed variables
    figure(3)
    plot(XTf(:,2),XTf(:,1),'-b',XTb(:,2),XTb(:,1),'-b')
    hold on
    sp = 0.02;
    text(1+sp,1, 'ProPro');
    text(0-0.10,0, 'Water');
    text(1+sp,0, 'ProAc');
    text(0-0.10,1, 'ProOH');
    axis([0 1 0 1])
    xlabel('XT');
    ylabel('XT');

end

Xf_end
Xb_end
T_end

============================================================================

function dXdtau =
                  fun_kineticRCM_for(tau,X,A,RP,Q,UA,UB,Properties,nij,P,R,
                  Da,nu)

% This function describes the forward path of the RCM. It uses the liquid
% composition vector and calculates the VLE of the system at this
% composition.
% Returns the differential equation of the forward path of the RCM. It
% describes the change of the liquid composition in time.

for i=1:4
    if X(i) < 0.00001;
        X(i)=0;
    end
end

X = X./sum(X);

% Calculation of the vapor composition in equilibrium with the liquid
[Y T] = vapor_comp(X,A,RP,Q,UA,UB,Properties,nij,P,R);

k1 = 7.060E6*exp(-66520/(R*T));
k1_ref = 7.060E6*exp(-66520/(R*360.75));
Keq = 0.7734*exp(9827/(R*T));

GAMMA = UNIQUAC(T,Q,X,RP,UA,UB);

% Differential equation describing the forward liquid composition in time
dXdtau = X-Y'+nu'*Da*(k1/k1_ref)*(GAMMA(2)*X(2)*GAMMA(3)*X(3)-
         GAMMA(1)*X(1)*GAMMA(4)*X(4)/Keq);
end

============================================================================
```

```
function dXdtau =
                  fun_kineticRCM_back(tau,X,A,RP,Q,UA,UB,Properties,nij,P,R
                  ,Da,nu)

% This function describes the backward path of the RCM. It uses the liquid
% composition vector and calculates the VLE of the system at this
% composition.
% Returns the differential equation of the backward path of the RCM. It
% describes the change of the liquid composition in time.

for i=1:4
    if X(i) < 0.00001;
        X(i)=0;
    end
end

X = X./sum(X);

% Calculation of the vapor composition in equilibrium with the liquid
[Y T] = vapor_comp(X,A,RP,Q,UA,UB,Properties,nij,P,R);

k1 = 7.060E6*exp(-66520/(R*T));
k1_ref = 7.060E6*exp(-66520/(R*360.75));
Keq = 0.7734*exp(9827/(R*T));

GAMMA = UNIQUAC(T,Q,X,RP,UA,UB);

% Differential equation describing the backward liquid composition in time
dXdtau = Y'-X+nu'*Da*(k1/k1_ref)*(GAMMA(2)*X(2)*GAMMA(3)*X(3)-
         GAMMA(1)*X(1)*GAMMA(4)*X(4)/Keq);

end
```